

REPORT 1369

BLOWING-TYPE BOUNDARY-LAYER CONTROL AS APPLIED TO THE TRAILING-EDGE FLAPS OF A 35° SWEEP-WING AIRPLANE¹

By MARK W. KELLY, SETH B. ANDERSON, and ROBERT C. INNIS

SUMMARY

A wind-tunnel investigation was made to determine the effects on the aerodynamic characteristics of a 35° swept-wing airplane of applying blowing-type boundary-layer control to the trailing-edge flaps. Flight tests of a similar airplane were then conducted to determine the effects of boundary-layer control on the handling qualities and operation of the airplane, particularly during landing and take-off.

The wind-tunnel and flight tests indicated that blowing over the flaps produced large increases in flap lift increment, and significant increases in maximum lift. The use of blowing permitted reductions in the landing approach speeds of as much as 12 knots.

INTRODUCTION

Numerous investigations have demonstrated that it is possible to significantly increase the lift of a wing by ejecting a high-velocity jet of air over the upper surface of a trailing-edge flap (e. g., refs. 1 and 2). These investigations have also indicated that the flow required to develop these lifts was so large that a powerful (and heavy) pumping system was required, and this deterred application of this system to actual aircraft. The introduction of the turbojet engine, which provided a convenient source of high-pressure air, and the trend of high-speed wing design to configurations having poor low-speed capabilities caused a renewal of interest in this method of obtaining high lift. The investigation reported in reference 3 indicated that the momentum of the jet, rather than the quantity flow, was the parameter which determined the effectiveness of blowing boundary-layer control, and that significant reductions in flow quantity requirements could be obtained by using high-pressure air (i. e., high jet velocities). It was also pointed out in reference 3 that sufficient amounts of high-pressure air to satisfy the requirements of a blowing flap could be bled from the compressor of a turbojet engine. However, the thrust of a turbojet engine diminishes rapidly as the amount of bleed air is increased; it was therefore considered desirable to investigate the possibilities of reducing the flow requirements by careful design of the flap and nozzle itself, so that the desired lift would be obtained for a minimum expenditure of jet momentum.

The primary purpose of the full-scale wind-tunnel tests reported herein was to investigate a blowing flap configuration which preliminary small-scale tests had indicated should

require less jet momentum to prevent flow separation than the arrangements previously investigated. Also, since the justification for presenting blowing flap effectiveness in terms of jet momentum was largely empirical, it was desired to verify this concept over the range of pressure ratios obtainable from current turbojet engines. Finally, it was desired to obtain sufficient data to design a blowing flap system into a research airplane for further study in flight.

The main purposes for conducting the flight tests were to investigate (1) the manner in which the pilots used the lift gains provided by the blowing flaps, and (2) the effects of boundary-layer control on the flying qualities and operation of the airplane.

This report presents results of both the wind-tunnel and flight investigations. Six-component force data showing the effects of blowing boundary-layer control on the longitudinal and lateral stability and control characteristics are discussed. Also presented are pilots' opinions of the effects of boundary-layer control on the handling qualities and operation of the airplane. Finally, the results of computations showing the effects of boundary-layer control on the landing and take-off performance are presented.

NOTATION

a	velocity of sound, ft/sec
A	area, sq ft
b	wing span, ft
c	wing chord parallel to plane of symmetry, ft
\bar{c}	mean aerodynamic chord, $\frac{2}{S} \int_0^{b/2} c^2 dy$
C_D	drag coefficient, $\frac{\text{drag}}{qS}$
C_L	lift coefficient, $\frac{\text{lift}}{qS}$
ΔC_L	increment of lift coefficient due to flaps
$C_{L_{max}}$	maximum lift coefficient
C_m	pitching-moment coefficient, $\frac{\text{pitching moment}}{qS\bar{c}}$
C_Q	flow coefficient, $\frac{W}{wVS}$
C_μ	momentum coefficient, $\frac{W/g}{qS} V$
$C_{L_{\delta_1}}$	rate of change of lift coefficient with flap deflection for full wing-chord flap (given as $C_{L_{\delta_1}}$ in ref. 5)

¹ Summarizes NACA Research Memorandums A65109 by Mark W. Kelly and William H. Tolhurst, Jr., and A66G30 by Seth B. Anderson, Hervey C. Quigley, and Robert C. Innis.

d	distance from engine thrust line to moment center, positive when thrust line is above moment center, ft
F_G	gross thrust from engine, lb
F_N	net thrust from engine, lb
g	acceleration of gravity, ft/sec ²
h_s	nozzle height, in.
M_j	jet Mach number, $\frac{V_j}{a}$
N	engine speed, rpm
p	free-stream static pressure, lb/sq ft
p_a	total pressure in flap duct, lb/sq ft
p_c	compressor discharge total pressure, lb/sq ft
P_d	duct pressure coefficient, $\frac{p_a - p}{q}$
q	dynamic pressure, lb/sq ft
S	wing area, sq ft
T	temperature, °R
V	free-stream velocity, ft/sec
V_i	indicated airspeed, knots
V_j	jet velocity assuming isentropic expansion,
	$\sqrt{\frac{2\gamma}{\gamma-1} RT_d \left[1 - \left(\frac{p}{p_a} \right)^{\frac{\gamma-1}{\gamma}} \right]}$, ft/sec
V_s	velocity at stall, knots
$V_{s\sigma}$	velocity at stall in glide condition, knots
\dot{W}	bleed air flow, lb/sec
w	specific weight of air at free-stream conditions, lb/cu ft
x	distance along airfoil chord normal to wing quarter-chord line, in.
y	spanwise distance perpendicular to plane of symmetry, ft
z	height in inches above wing reference plane defined by quarter-chord line and the chord of the wing section at $0.663b/2$
Λ	sweep angle, deg
α	angle of attack of fuselage reference line, deg
δ	ratio of total pressure at compressor inlet to standard pressure at sea level
δ_f	flap deflection, measured normal to flap hinge line (given as δ in ref. 5), deg
$\bar{\delta}_f$	flap deflection, measured in plane parallel to plane of symmetry (given as δ in ref. 5), deg
δ_H	horizontal-tail deflection, deg
ϵ	angle between engine thrust axis and fuselage reference line, deg
γ	ratio of specific heats for air, 1.4
θ	ratio of total temperature at compressor inlet to standard temperature at sea level
φ	angular distance between flap nozzle and a line drawn through the flap hinge line perpendicular to the wing chord plane (fig. 18)

SUBSCRIPTS

d	flap duct
f	flaps
j	flap jet
u	uncorrected

DESCRIPTION OF RESEARCH AIRPLANES, INSTRUMENTATION, AND TESTS

WIND-TUNNEL AIRPLANE AND INSTRUMENTATION

Airplane.—The wind-tunnel tests were conducted on a F-86D airplane on which the normal single-slotted flaps had been replaced by blowing flaps. A photograph showing the general arrangement of the airplane installed in the Ames 40- by 80-foot wind tunnel is presented in figure 1. The major dimensions and parameters of aerodynamic importance are shown in figure 2. The airfoil section at the wing root was an NACA 0012-64 (modified) and at the wing tip, an NACA 0011-64 (modified). The ordinates of the airfoil sections are given in table I. Detailed information for the wing and flaps is given in figure 3. Static-pressure orifices were installed in the afterportion of the flap upper surface so that the degree of flow separation could be estimated.

Flap nozzles.—Two flap and nozzle configurations were tested in the wind-tunnel investigation. The first of these was a plain flap arrangement in which the nozzle was essentially a slit in the flap upper surface extending over the full span of the flap. A section view of the nozzle is shown in figure 3. The nozzle blocks were machined from cold-rolled mild-steel stock and were fastened to the top wall of the flap duct with countersunk machine screws. Various nozzle heights were obtained by shimming the forward nozzle block. This assembly was made rigid enough to hold the nozzle deflections, under load, to acceptable values

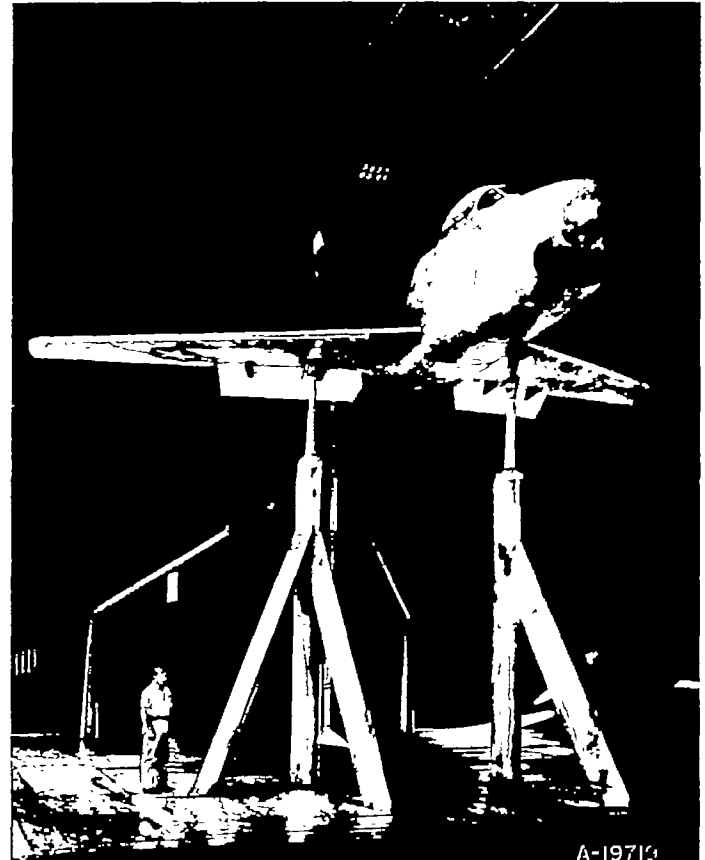
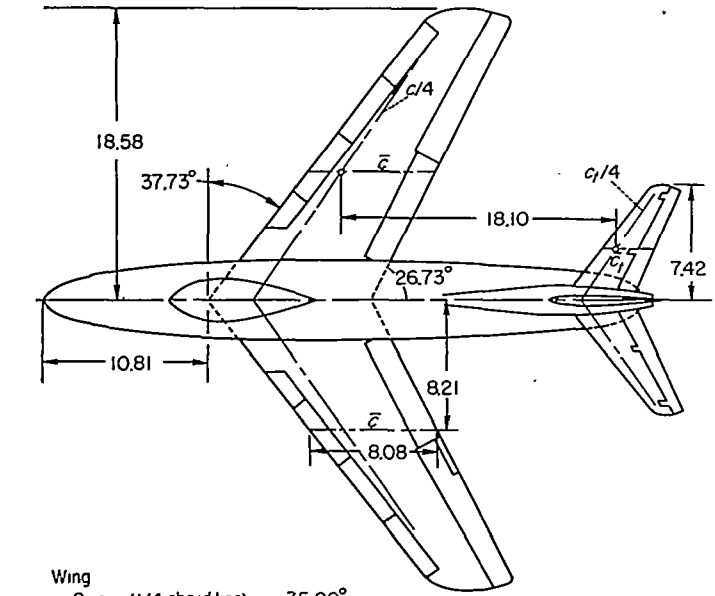


FIGURE 1.—Photograph of the F-86D airplane mounted in the Ames 40- by 80-foot wind tunnel.



Wing	
Sweep (1/4 chord line)	35.00°
Aspect ratio	4.79
Taper ratio	.51
Twist	2.0°
Dihedral	3.0°
Area	287.9 sq ft
Incidence (root)	1.0°
Horizontal tail	
Sweep	35.00°
Aspect ratio	4.73
Taper ratio	.45
Twist	0°
Dihedral	0°
Area	46.5 sq ft

All dimensions in feet unless otherwise noted

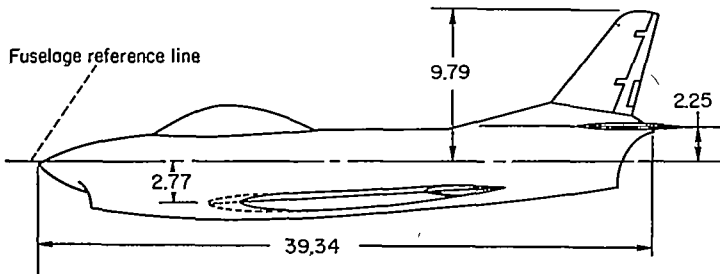


FIGURE 2.—General arrangement of the F-86D airplane.

without the use of fasteners or spacers in the high-velocity portion of the nozzle. For part of the investigation, spacers were simulated by cementing small rectangular pieces of gasket material at regular intervals in the nozzle.

In order to investigate the effects of chordwise location of the nozzle on the effectiveness of the flap, the flap duct was constructed so that it could be rotated about the flap hinge line independently of the flap itself. For most of the investigation the nozzle was located at an angular setting (ϕ) equal to one-half the flap deflection.

The second flap and nozzle arrangement investigated had a single-slotted flap and a nozzle located in the wing shroud ahead of the flap similar to the configuration investigated in reference 3. Details of this flap and nozzle are shown in figure 4.

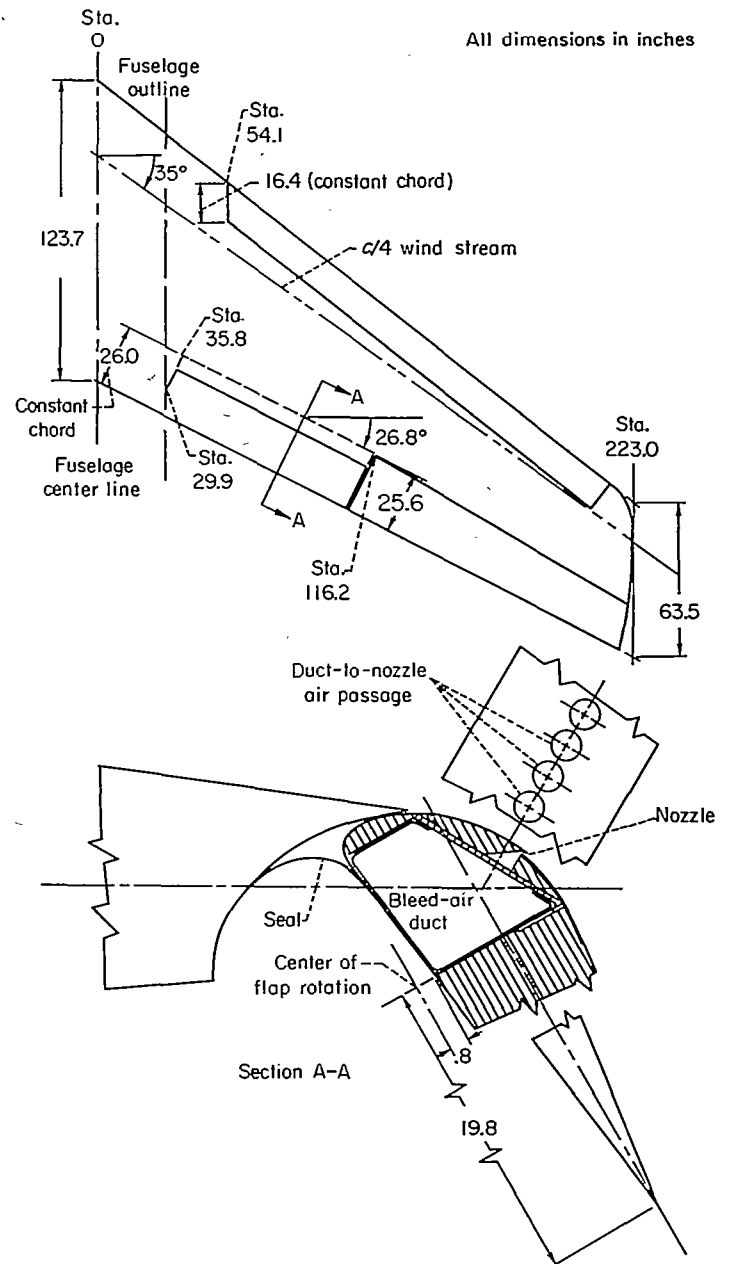


FIGURE 3.—Details of wing and plain blowing flap.

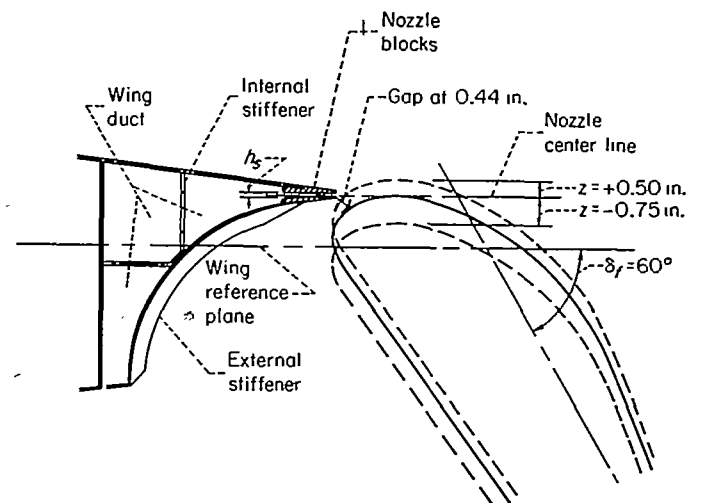


FIGURE 4.—Details of shroud blowing flap.

Engine and ducting.—For these tests the J-47 turbojet engine normally used in this airplane was replaced by a J-34 engine. (This was done only because spare J-47 engines were not available.) The amount of air delivered to the flaps was controlled by a butterfly valve in each duct.

The weight rate of flow to each flap was determined from total pressure, static pressure, and temperature measurements in the ducts. This system was calibrated using a thin plate orifice. The total-pressure and temperature measurements used for calculating the jet momentum were taken at the entrance of the flap duct. Static-pressure and temperature measurements were also made at the outboard end of the flap duct to obtain an estimate of the spanwise variation of the jet momentum.

TESTS

Range of variables.—The investigation covered a range of angles of attack from -2° to $+23^\circ$ and Reynolds numbers from 5.8 to 10.1×10^6 . These Reynolds numbers were based on the mean aerodynamic chord of the airplane (8.08 ft) and correspond to free-stream dynamic pressures from 15 to 55 pounds per square foot. The range of flap deflections investigated was from 45° to 85° . The airplane was tested with and without the horizontal tail, and with and without the leading-edge slats extended.

Method of testing.—To define completely the aerodynamic characteristics of the airplane as a function of flap jet momentum, it would have been necessary to obtain data for various jet momentum flows throughout the angle-of-attack range. However, in order to expedite the tests, the momentum flow was varied at only three angles of attack, 0° , 8° , and 12° . (The angle of attack for maximum lift with leading-edge slats retracted was near 12° .) The additional information required to obtain typical lift, drag, and pitching-moment data for the airplane was obtained by testing at several other angles of attack with a constant jet momentum well above that required for flow attachment.

CORRECTIONS

The force data obtained from the wind-tunnel balance system were not corrected for support-strut interference but were corrected for the effects of the wind-tunnel-wall interference as follows:

$$\alpha = \alpha_u + 0.611 C_{L_u}$$

$$C_D = C_{D_u} + 0.0107 C_{L_u}^2$$

$$C_m = C_{m_u} + 0.00691 C_{L_u} \quad (\text{for tail-on tests only})$$

The following corrections for the effects of the engine thrust were made:

$$C_L = \frac{\text{total lift}}{qS} - \frac{F_N}{qS} \sin(\alpha + \epsilon)$$

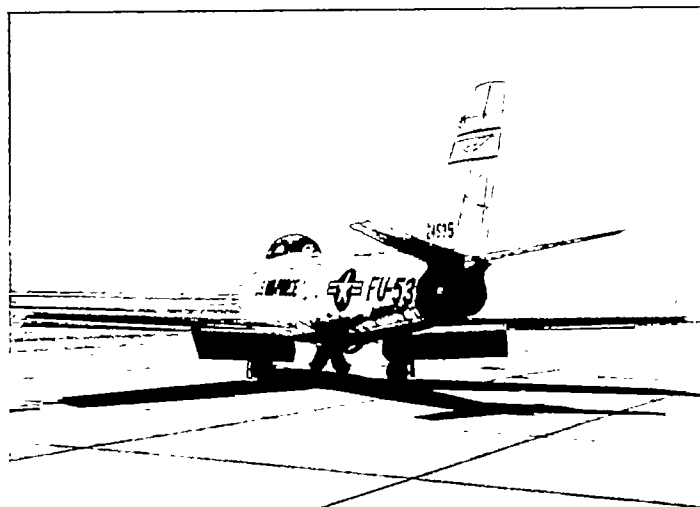
$$C_D = \frac{\text{total drag}}{qS} + \frac{F_N}{qS} \cos(\alpha + \epsilon)$$

$$C_m = \frac{\text{total moment}}{qSc} + \frac{F_N d}{qSc}$$

FLIGHT TEST AIRPLANE

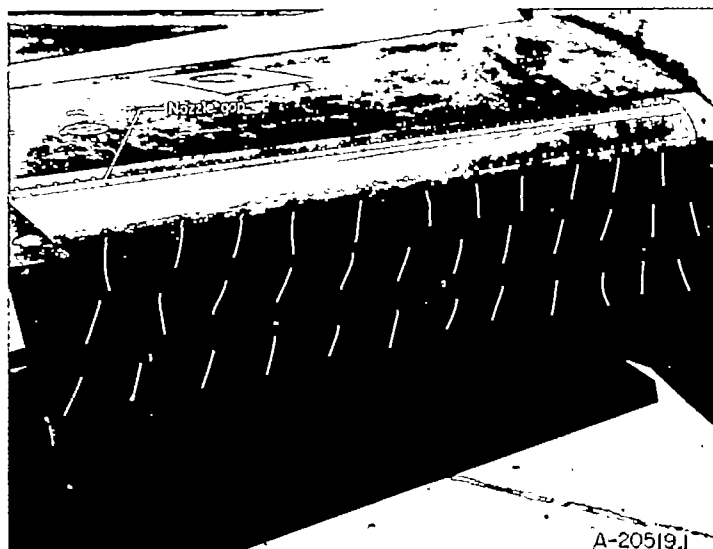
The flight tests were conducted with an F-86F airplane on which the standard single-slotted flaps were replaced by blowing flaps. Pertinent dimensions of the airplane are given in table II. A general view of the airplane and a close-up of the flap are presented in figures 5 and 6, respectively. The blowing system consisted of a manifold to collect air from the last stage of the engine compressor of the J-47 engine, a butterfly valve controlled by the pilot, and a 3-inch-diameter ducting to each flap. The ducting was mounted on the underside of the fuselage to facilitate installation.

The flap used for the blowing system was a plain type made by reworking the nose section of the slotted flaps normally used on the airplane. The flap tracks were removed and external hinge brackets were installed on the undersurface of the wing, allowing flap deflections up to 66° . A rotating O-ring-type seal was used to supply air to the flap at a point on the center of flap rotation. A sketch of the



A-20518

FIGURE 5.—General view of test airplane.



A-20519.1

FIGURE 6.—Close-up of flap.

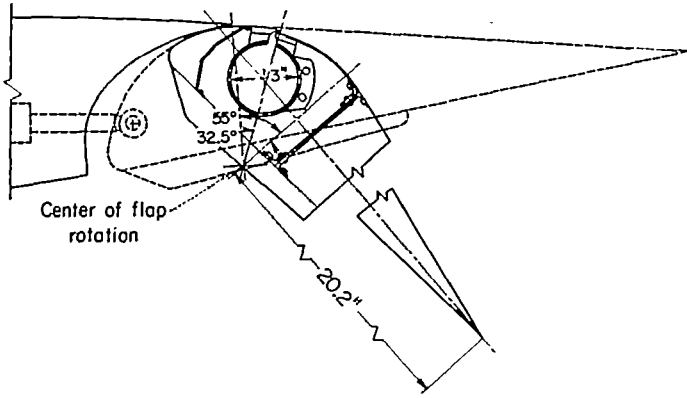


FIGURE 7.—Details of blowing flap construction for flight airplane.

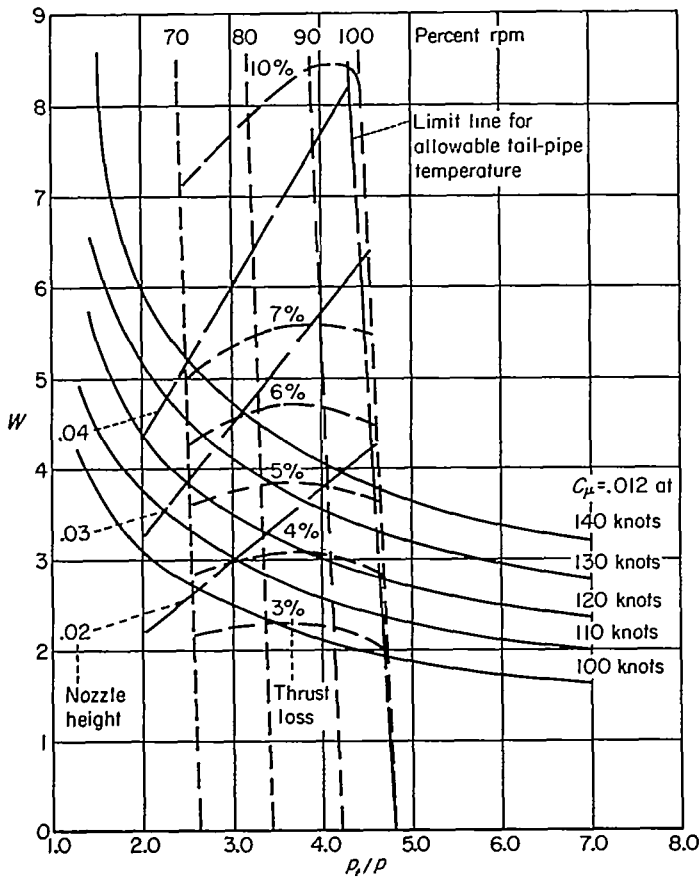


FIGURE 8.—Illustration of analysis for selecting proper nozzle size for blowing flap.

flap cross section is given in figure 7. All parts of the air-supply system were made of steel. The nozzle block was made in two parts, the lower part of steel welded to the 3-inch-diameter tubing, the upper part forming the nozzle exit of 2024-T aluminum, fastened by screws to the steel nozzle block. Spacers were used at 3-inch-span intervals to provide a 0.020-inch nozzle gap. The area of the nozzle was 0.0221 square feet.

It should be noted that the nozzle area was not selected arbitrarily, but was carefully chosen to meet the flow requirements of the blowing flaps and the limitations of bleed air from the engine. Figure 8 indicates graphically how this selection was made. First, the weight rate of flow available from the engine bleed air system was plotted as a function of

pressure ratio for various engine speeds. These are the dashed lines in figure 8. Curves representing the jet momentum required to give the desired flap lift were then superimposed on this same plot. These are the hyperbolic-shaped solid curves in figure 8 and were obtained from the equation

$$W = \frac{C_p g q S}{M_j (a_j/a_a) \sqrt{\gamma R T_a}}$$

The value of C_p used was 0.012, which the wind-tunnel investigation indicated to be about 14 percent above that required to prevent flow separation with the flap deflected 60°. The values of dynamic pressure used correspond to flight speeds of 100 to 140 knots, the range of interest in the landing approach. Finally, the weight rate of flow which can be driven through nozzles of various size was computed and is shown in figure 8 by the long dash lines. These were developed from the equation.

$$W = g \rho_a a_a \left(\frac{\rho}{\rho_a}\right) \left(\frac{a}{a_a}\right) A_j$$

where $\rho/\rho_a = 0.634$ and $a/a_a = 0.913$ for air flow in choked nozzles.

It is seen from figure 8 that, to have the flap fully effective for landing approach conditions (say 70- to 80-percent rpm and 100 to 120 knots) a nozzle height of 0.02 to 0.03 inch should be used. For a nozzle height of 0.02 inch, a loss of maximum thrust of between 5 and 6 percent due to bleeding air from the engine would be anticipated.

The weight of the boundary-layer-control equipment for this research-type installation was 175 pounds. In a production-type installation a considerable savings in weight should be possible.

The amount of engine bleed air actually used at various engine speeds is presented in figure 9. These values of bleed air correspond to approximately 3.5 percent of the primary engine air flow. The bleed flow quantity was calcu-

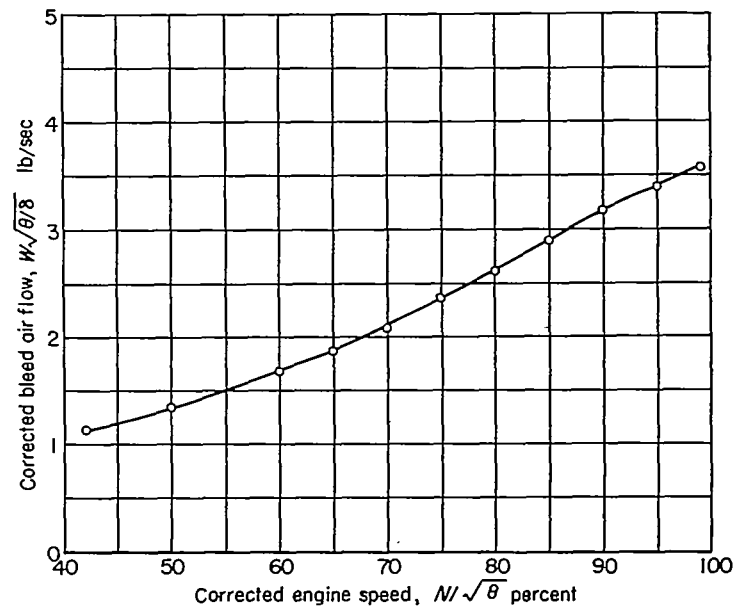


FIGURE 9.—Variation of engine bleed with engine speed; sea level, J-47 engine.

lated from one-dimensional flow equations using measured values of pressure, temperature, and nozzle area. The variation of static thrust (measured on a thrust stand) with percent engine speed is presented in figure 10 with and

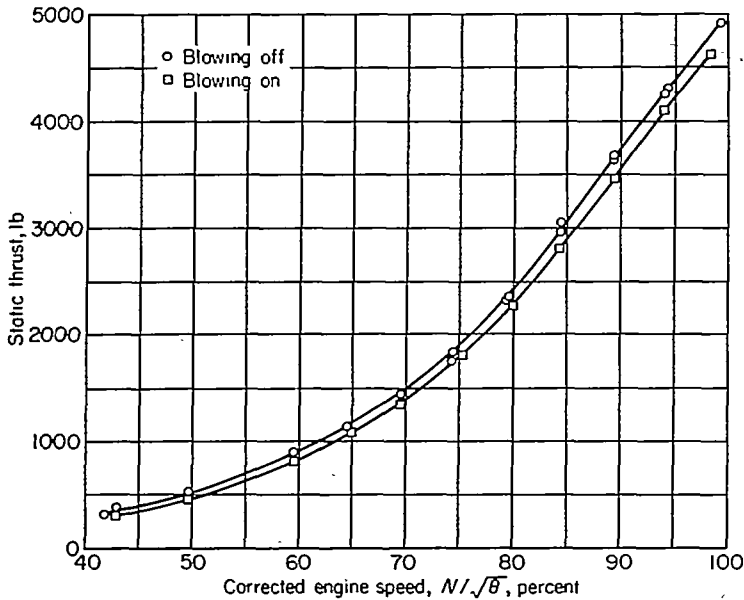


FIGURE 10.—Variation of static thrust with engine speed for blowing on and off; sea level, J-47 engine.

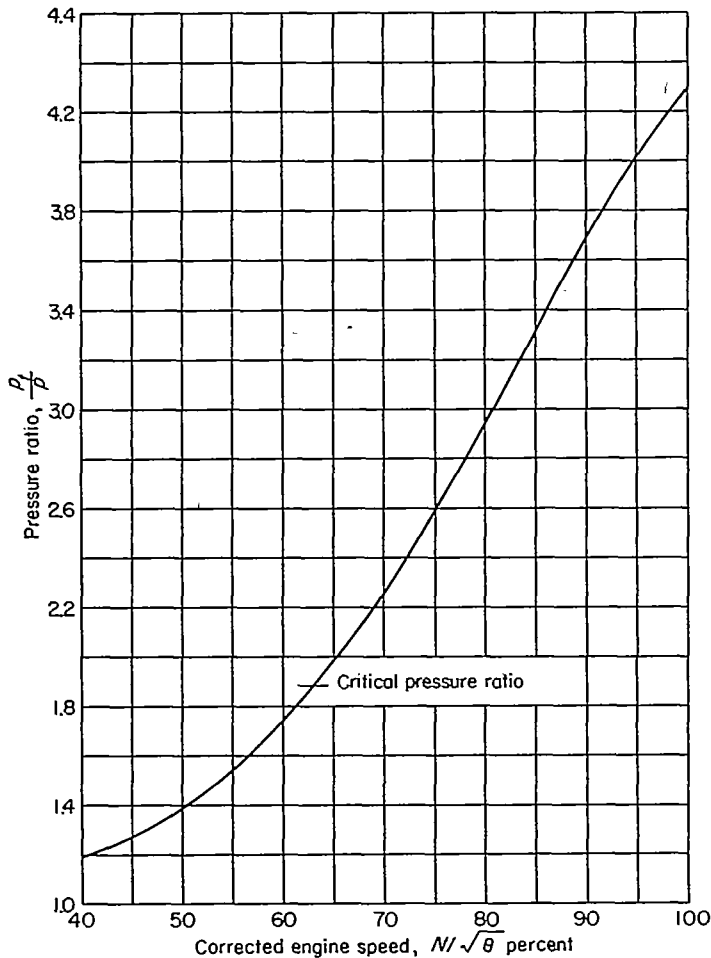


FIGURE 11.—Variation of pressure ratio at engine bleed ports with engine speed; J-47 engine.

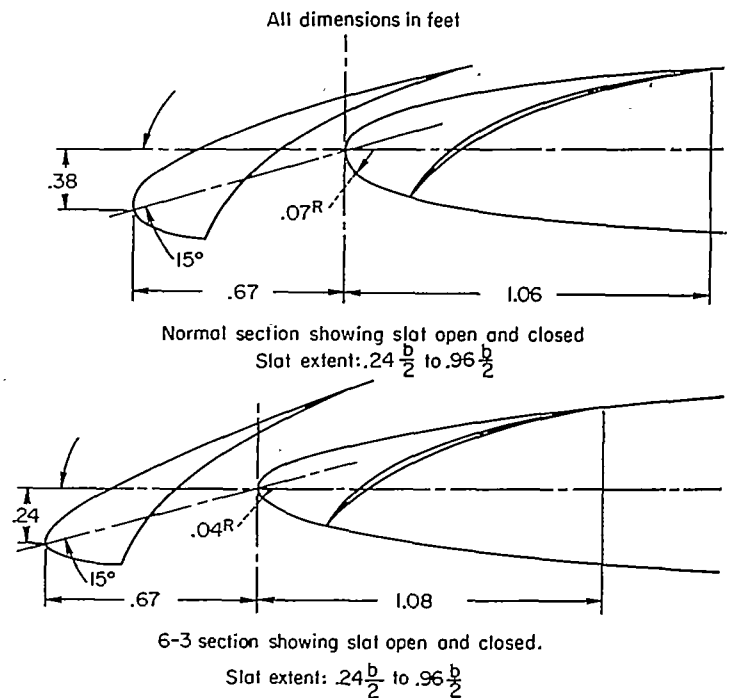


FIGURE 12.—Cross sections normal to wing leading edge of the normal slat and the 6-3 slat.

without bleed air extraction. It can be noted that for the blowing-on case there was a reduction in static thrust of approximately 5 percent. The variation of pressure ratio with percent engine speed is presented in figure 11. It will be noted that sonic flow would occur in the nozzle exit at approximately 63-percent rpm.

Standard NACA instruments were used to record airspeed, altitude, acceleration, duct pressures, and angle of attack. Values of airspeed, altitude, and angle of attack were measured approximately 8 feet ahead of the fuselage nose. Duct pressures in the flaps were measured at the midspan station of the flaps.

The flight tests were conducted with two wing leading-edge configurations, an F-86D type slat, and a 6-3 slat.² A sketch of the cross section of each leading-edge device is shown in figure 12. The majority of data obtained in the flight investigation was with the 6-3 slat, since this is the leading edge currently used with F-86F type airplanes.

Tests were conducted at sea level and 5,000 feet over a speed range from 170 knots to the stall. An average wing loading of 45.5 pounds per square foot was used with the take-off center of gravity at 24.1 and 26.6-percent mean aerodynamic chord for the airplane with the F-86D slatted leading edge and 6-3 leading edge, respectively. The engine rpm was held fixed for a given series of test runs. Tests were conducted at trailing-edge flap deflections of 38°, 45°, 55°, 60°, and 66°.

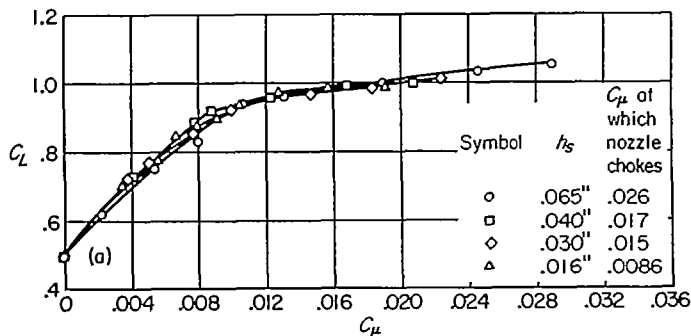
RESULTS AND DISCUSSION

WIND-TUNNEL TESTS

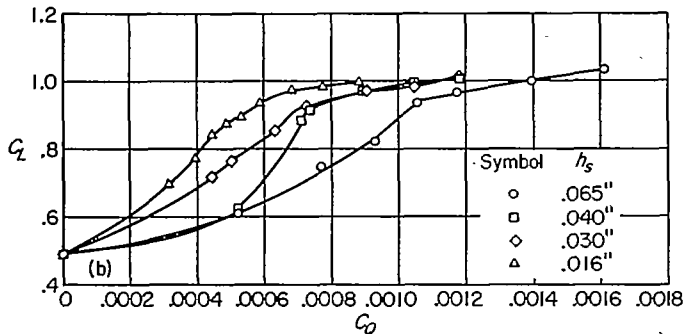
Correlation of blowing-flap performance with momentum coefficient.—One of the first objectives of the test programs was to establish whether the effectiveness of a partic-

² The designation "6-3" refers to a full-span chord extension of 6 inches at the wing root and 3 inches at the wing tip.

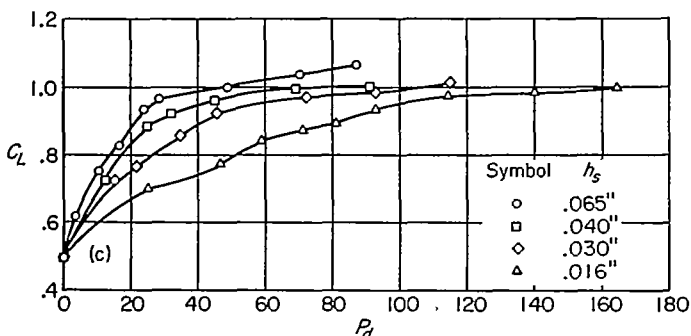
ular blowing-flap configuration was determined solely by the momentum of the air ejected over the flap. This was done by making a series of tests on the same basic flap configuration with various nozzle openings. Typical results of these tests are presented in figure 13 (a). It should be noted that, although the nozzle opening was changed from a value of 0.016 inch to 0.065 inch (corresponding to values of h_s/c from 0.00017 to 0.00067), good correlation with momentum coefficient is obtained. The data presented in figure 13 (a) cover a range of nozzle pressure ratios from subcritical up to 2.9, and therefore a range of expanded jet velocities from subsonic to supersonic. It should be noted that no particular aerodynamic difficulties or benefits are associated with either subsonic or supersonic jet velocities. Corresponding variations of lift coefficient with flow coefficient and duct pressure coefficient are shown in figures 13 (b) and 13 (c), respectively. Here it is seen that the effects of nozzle height are significant, and that values of flow coefficient or pressure coefficient have meaning only when the nozzle height is specified. While



(a) Variation of lift coefficient with momentum coefficient.



(b) Variation of lift coefficient with flow coefficient.



(c) Variation of lift coefficient with duct pressure coefficient.

FIGURE 13.—Effect of nozzle height on the flow requirements of the blowing flap; $\delta_f = 60^\circ$, $\alpha_w = 0^\circ$, $R = 7.5 \times 10^6$, tail off.

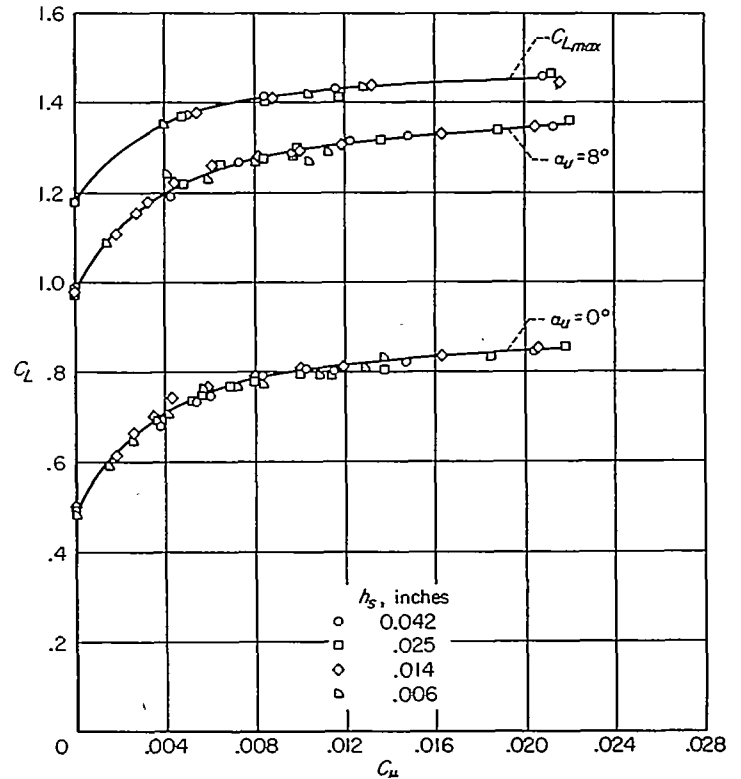
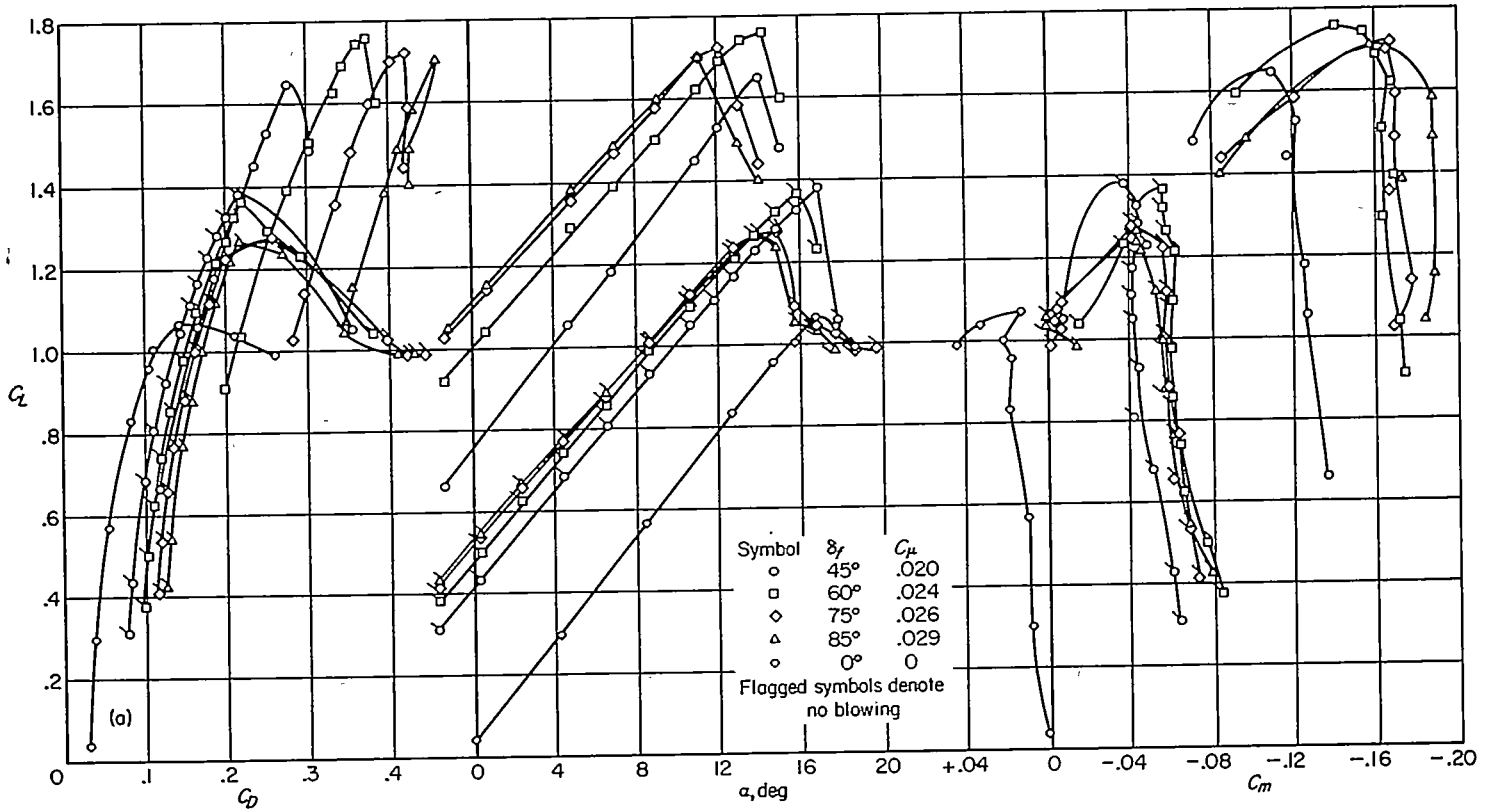


FIGURE 14.—Effect of nozzle height on the flow requirements of the blowing flap of reference 4; $\delta_f = 60^\circ$, $R = 10.7 \times 10^6$.

the data presented in figure 13 are for 0° angle of attack only, similar results were obtained at 8° and 12° angle of attack. Figure 14 presents similar results obtained from later wind-tunnel tests of an F-93 airplane equipped with similar blowing flaps (ref. 4). Here the range of nozzle pressure ratios used was from subcritical up to 9.5, and good correlation of C_L with C_{μ} was again obtained. Thus, it appears that, for pressure ratios obtainable from turbojet engine bleed-air systems, the effects of blowing boundary-layer control on flap lift are adequately defined by the jet momentum.

Typical effects of blowing on aerodynamic characteristics.—Figure 15 (a) presents the tail-off lift, drag, and pitching-moment characteristics of the airplane with various flap deflections with and without blowing. The data obtained with blowing were taken at constant values of momentum coefficient which were more than sufficient to provide attached flow for each flap deflection. It is seen that blowing over the flap produced the type of lift and pitching-moment increments which would be expected from substantial increases in flap effectiveness. The drag coefficient for a given flap deflection was increased by blowing. This may be surprising in view of the fact that blowing over the flap should reduce the amount of flow separation and hence the profile drag of the flap. However, it must be remembered that the total airplane drag is the sum of both profile and induced drag. Since the total drag was increased by blowing, while the profile drag was decreased, it must be concluded that blowing over the flaps resulted in an increase in induced drag. The use of a short span, highly effective flap will usually cause a significant distortion of the wing span loading and a resulting increase in the induced drag of the wing. The order of magnitude of this induced drag can be

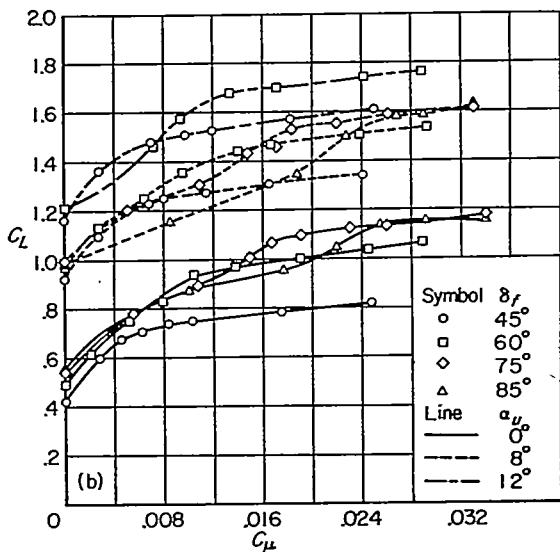


(a) Typical aerodynamic characteristics with and without blowing.

FIGURE 15.—Effects of blowing over the flaps on the aerodynamic characteristics of the airplane; $R=7.5 \times 10^5$, tail off, $h_s=0.065$ inch.

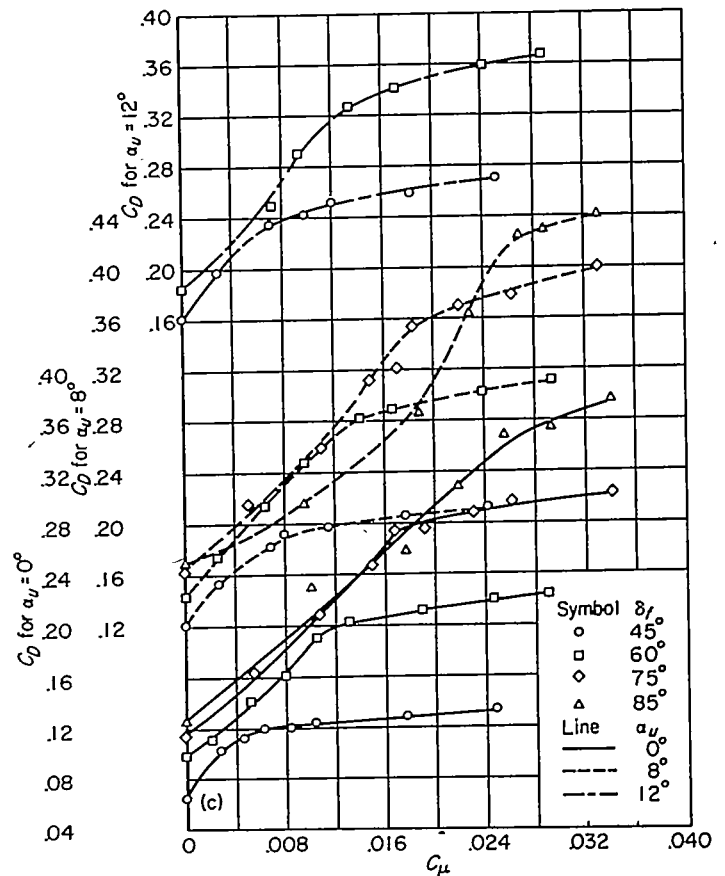
estimated from the theory of reference 5. It should be noted that this induced drag increment is a function of flap span and is more for small-span flaps than it is for large-span flaps.

The data presented in figure 15 were obtained with the flap nozzle located at an angular setting (φ) equal to one-half the flap deflection, as previously pointed out in the section "Wind-Tunnel Airplane and Instrumentation." This was done because previous research (ref. 6) had indicated that



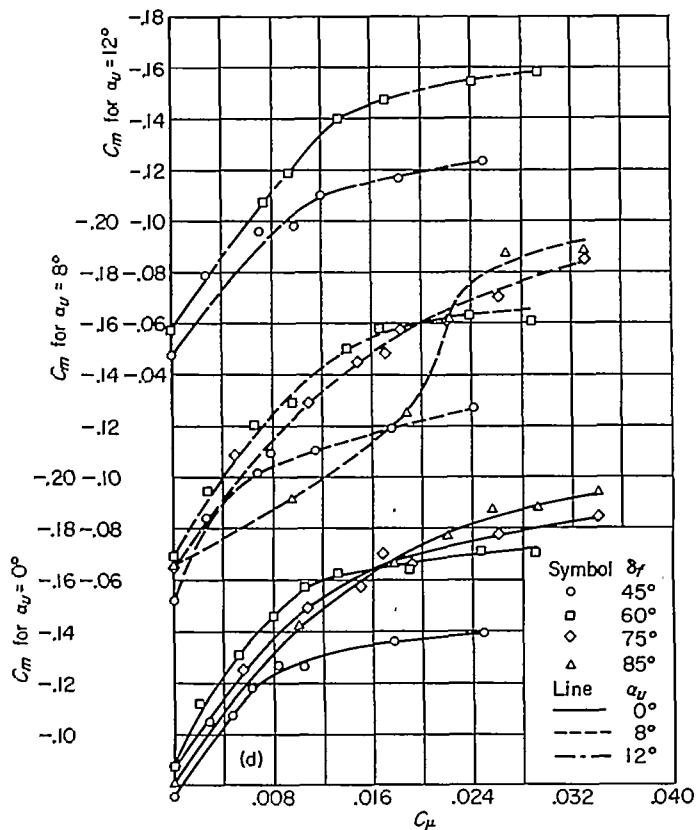
(b) Variation of lift coefficient with momentum coefficient.

FIGURE 15.—Continued.



(c) Variation of drag coefficient with momentum coefficient.

FIGURE 15.—Continued.



(d) Variation of pitching-moment coefficient with momentum coefficient.

FIGURE 15.—Concluded.

this setting would put the nozzle near the minimum-pressure point on the flap, and this was believed to be near the optimum location. Subsequent testing to determine the effects of nozzle location (see section entitled "Effect of Nozzle Location") indicated that this location was, in fact, near the optimum. However, the flap lift was relatively insensitive to nozzle position, and the data presented in figure 15 are typical of those which would be obtained with the nozzle located anywhere between the minimum-pressure point on the flap and the wing-flap juncture.

Figures 15 (b), (c), and (d) present the variation of lift, drag, and pitching-moment coefficient with momentum coefficient. As mentioned previously, the momentum coefficient was varied only at uncorrected angles of attack of 0°, 8°, and 12°. (The momentum coefficient was not varied at 12° angle of attack for flap deflections of 75° and 85° since, with these flap deflections, the wing had already passed maximum lift.) Figure 15 (b) shows that, as the momentum coefficient was increased, the lift at first increased rapidly, but then the rate of increase fell off to a relatively low value. Static-pressure measurements on the upper surface of the flap indicated that the initial rapid increase in lift was associated with the control of the boundary layer on the flap. The additional lift obtained after the flow was attached is due to wing circulation induced by the jet flow over the flap. The data presented in figure 15 (b) indicate that the momentum coefficient required for a given flap lift increment is relatively low when the flap deflection is large enough so that the desired lift is obtained by using

blowing primarily for boundary-layer control rather than to provide jet-induced circulation. It might be noted that the pitching moment per unit lift due to flap deflection is not significantly changed by blowing. This is shown in the following table which was obtained from the data presented in figures 15 (b) and 15 (d) for 0° uncorrected angle of attack:

δ_f	45°		60°		75°		85°	
C_μ	0	0.006	0	0.0105	0	0.0168	0	0.0255
$\frac{\Delta C_m}{\Delta C_L}$	-0.20	-0.18	-0.20	-0.18	-0.18	-0.17	-0.16	-0.17

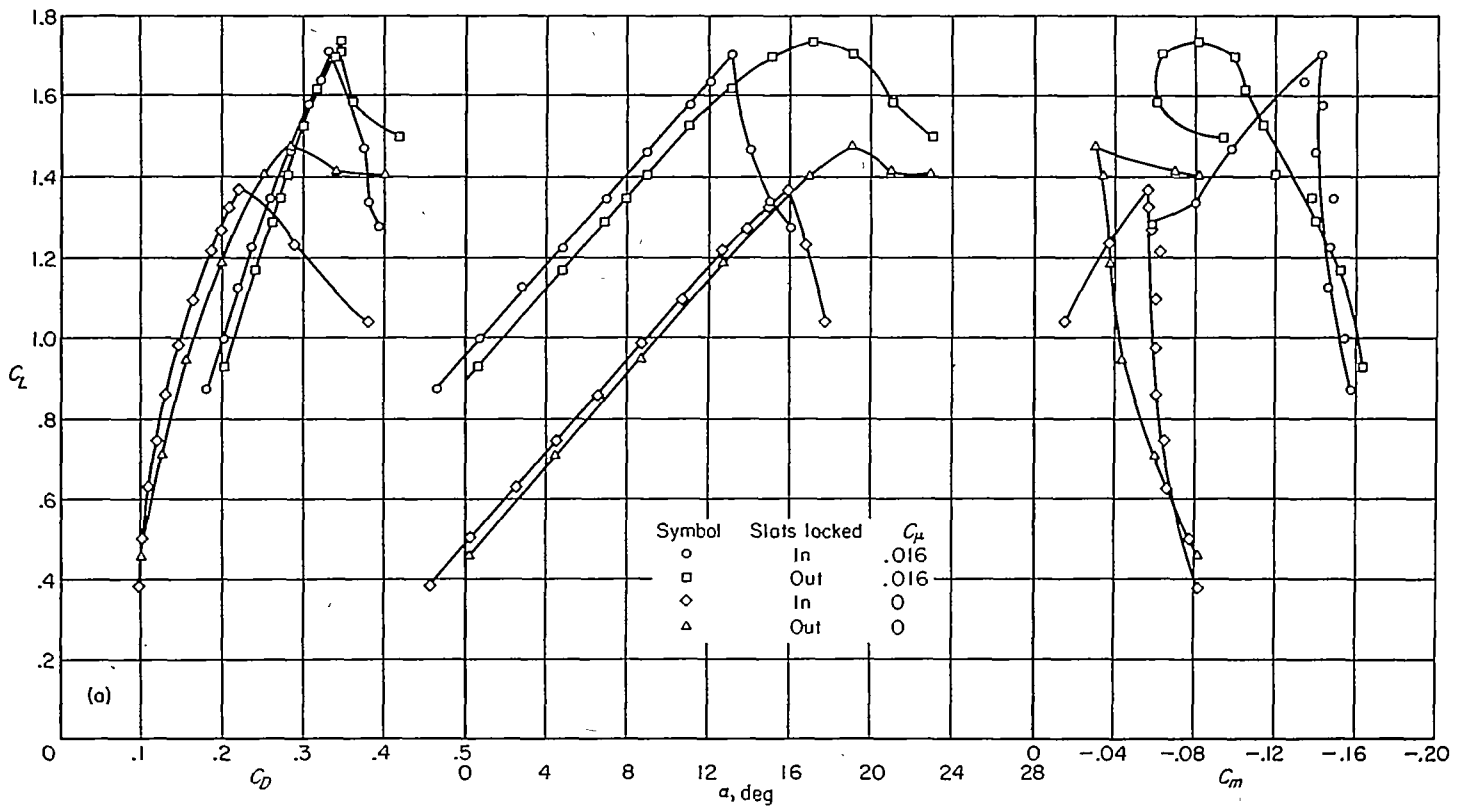
All of the preceding data were obtained at a Reynolds number of 7.5×10^6 . Results of this investigation showed no effect of Reynolds number on the lift increment due to blowing from $R=5.8$ to 10×10^6 .

Results of tests to determine the effects of blowing over the flaps on static lateral and directional stability indicated that both were slightly increased. It was also found that blowing over the flaps increased the aileron effectiveness by about 25 percent.

Effects of leading-edge slats.—Figures 16 (a) and (b) show the effects of extending the leading-edge slats on the aerodynamic characteristics of the airplane with and without blowing on the flaps. It is seen that extending the slats had no significant effect on the flap performance, that is, had no effect on the lift increment due to blowing or the required momentum coefficients. The loss in lift at angles of attack below maximum lift is due primarily to the nose camber effect of the slats. It should be noted that there is no nonlinearity in the lift curve such as that obtained with area-suction flaps in the investigation of reference 6, where the vortex shed from the slat root spoiled the flow over a portion of the flap. The leading-edge slats did not provide a significant increase in maximum lift, although they did change the type of stall from one that was very abrupt to one that was relatively gradual. The pitching-moment data show that, with blowing on, the leading-edge slats did not provide the stable variation in pitching moment at the stall that was obtained without blowing.

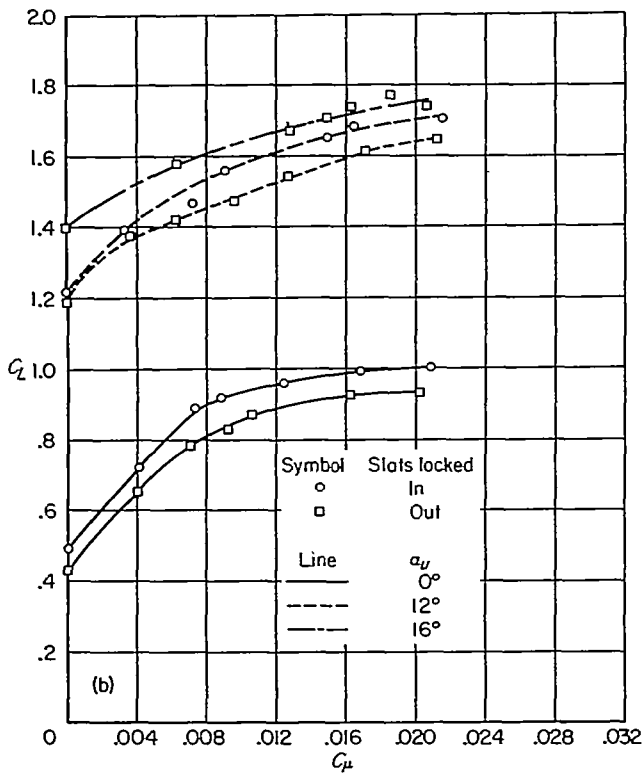
Effect of horizontal tail.—Lift and pitching-moment data for the airplane with and without the horizontal tail and with and without blowing on the flap are shown in figures 17 (a) and (b). It is seen that with the tail on and the airplane at a constant lift coefficient, blowing over the flap produced a positive pitching-moment change. This was caused by an increase in downwash in the vicinity of the horizontal tail. (The dynamic pressure at the tail was measured and found equal to free-stream dynamic pressure.)

Effect of nozzle location.—Figure 18 presents lift coefficient as a function of momentum coefficient for various nozzle locations on the flaps which were deflected 60°. The data indicate that, for the range of nozzle locations available with the flaps deflected 60°, no appreciable effect of nozzle location was found at angles of attack of 8° and 12°, which are in the range of most significance as far as landing and take-off of the airplane is concerned. Results from similar tests with the flaps deflected 85° showed that, with the nozzle behind the minimum pressure point ($\phi=62.5^\circ$), the flow could not be



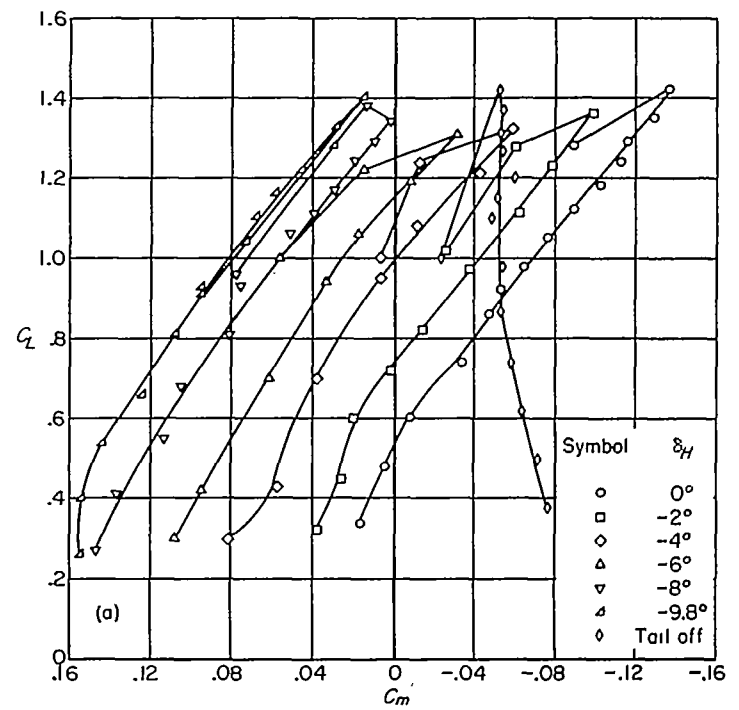
(a) Typical aerodynamic characteristics with and without leading-edge slats.

FIGURE 16.—Effects of leading-edge slats on the aerodynamic characteristics of the airplane with blowing over the flaps; $\delta_f=60^\circ$, $R=7.5 \times 10^6$ tail off, $h_s=0.040$ inch.



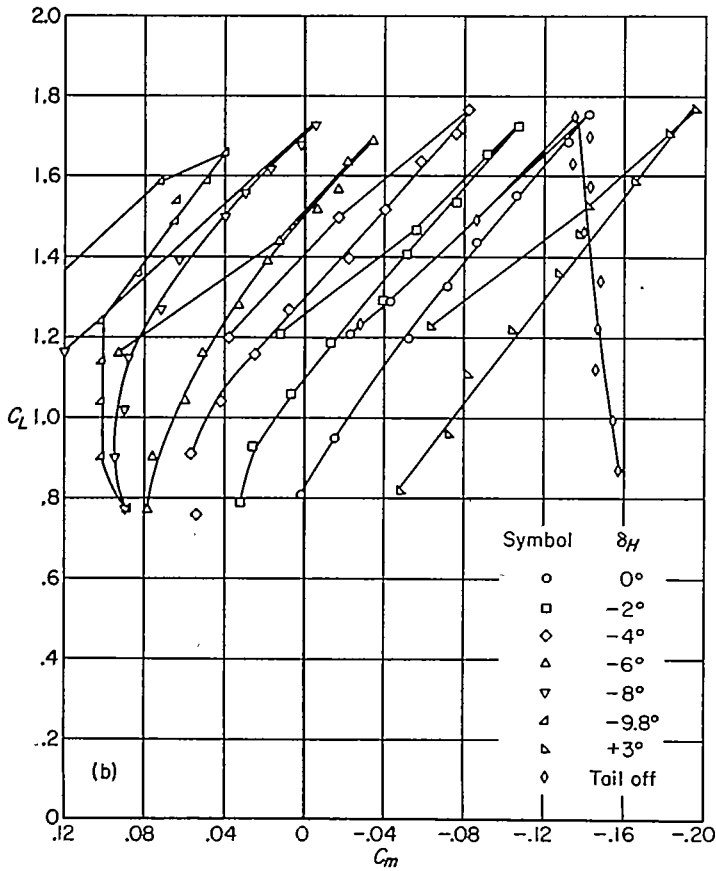
(b) Variation of lift coefficient with momentum coefficient.

FIGURE 16.—Concluded.



(a) Blowing off.

FIGURE 17.—Pitching-moment characteristics of the airplane with and without the horizontal tail.



(b) Blowing on.
FIGURE 17.—Concluded.

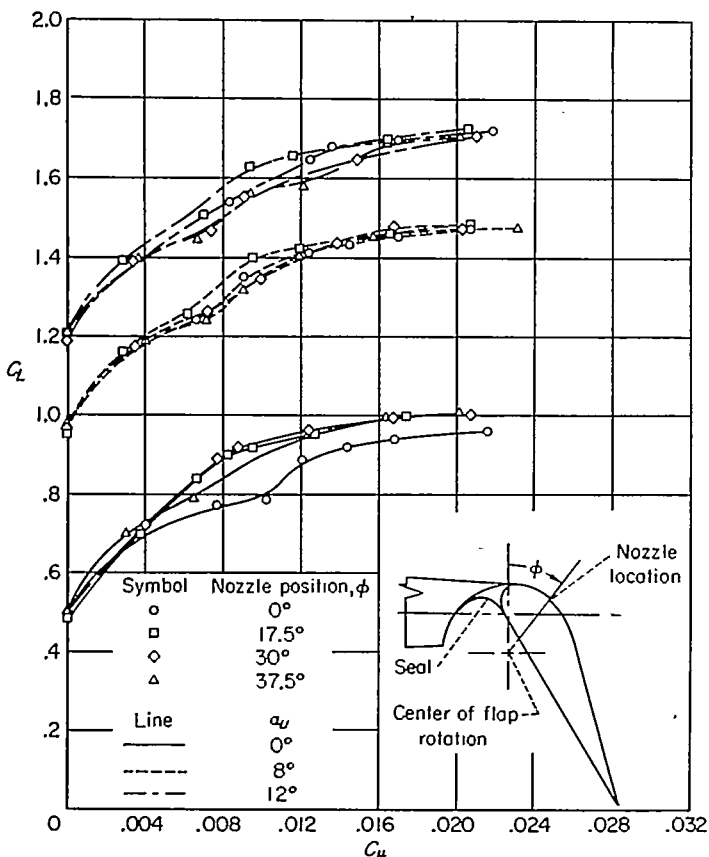


FIGURE 18.—Effect of nozzle position on the variation of lift coefficient with momentum coefficient with the nozzle in the flap upper surface; $\delta_f=60^\circ$, tail off, $R=7.5 \times 10^6$.

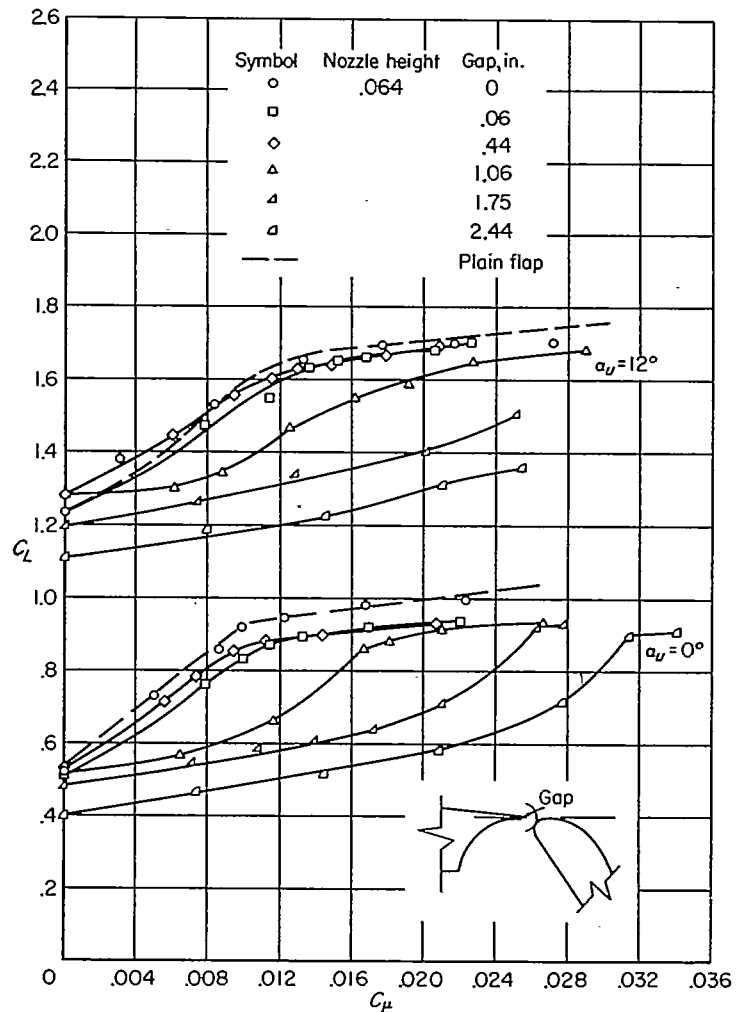


FIGURE 19.—Effects of flap position on the variation of lift coefficient with momentum coefficient for the nozzle located in the wing shroud; flap upper surface tangent to nozzle center line; $\delta_f=60^\circ$, tail off, $R=7.5 \times 10^6$.

attached with the highest value of momentum coefficient available. In general, these data indicate that, as long as the nozzle is located between the wing-flap juncture and the minimum-pressure point on the flap, no significant effect on flow requirements will be obtained. It should be noted that, for the case where the nozzle is fixed with respect to the flap, the nozzle should be positioned approximately at the location of the minimum-pressure point on the flap for the maximum flap deflection contemplated. At lower flap deflections the nozzle will then be ahead of the minimum-pressure point on the flap and satisfactory performance should be obtained.

Figure 19 shows similar results obtained from subsequent tests of this airplane with a blowing flap with the nozzle in the wing shroud. With this arrangement, it was found that to obtain the minimum jet momentum requirements, the flap should be positioned close to the nozzle (within 0.44 inch for this flap). At this optimum position, the variation of lift coefficient with momentum coefficient for the shroud blowing flap compares favorably with that for the plain blowing flap.

Effect of spacers in nozzle.—For this phase of the investigation the nozzle was plugged with rectangular spacers at regular spanwise intervals to simulate an interrupted nozzle, that is, several discrete nozzles along the flap span. Data

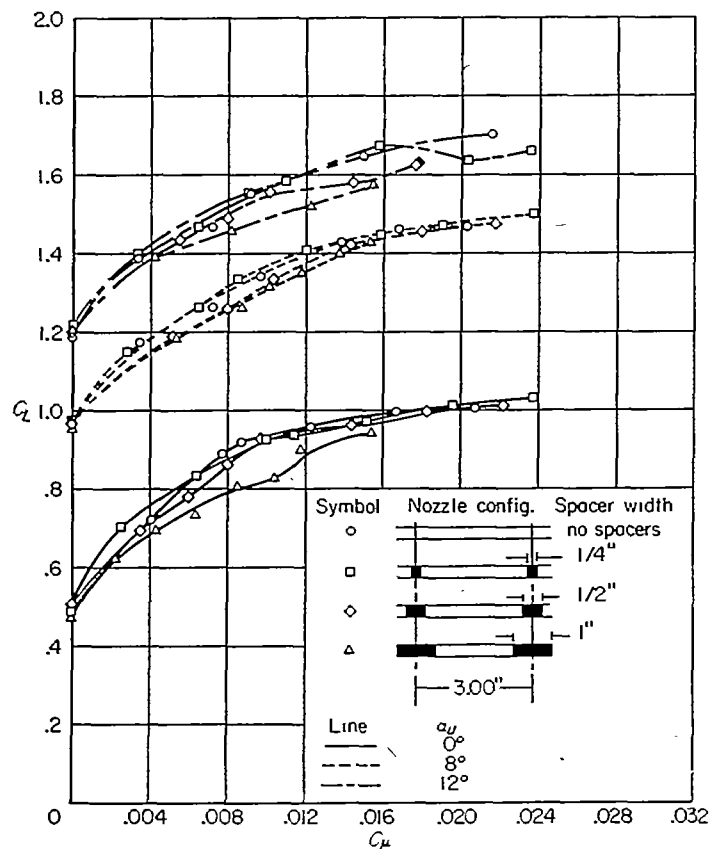


FIGURE 20.—Variation of lift coefficient with momentum coefficient for nozzles having various spacer arrangements; $\delta_f = 60^\circ$, $R = 7.5 \times 10^6$, tail off, $h_s = 0.040$ inch.

for various nozzle configurations are presented in figure 20. It is seen that no significant effect was obtained until nozzles 2 inches long separated by 1-inch spacers were simulated. For this arrangement, it was found that the required momentum coefficient for a given lift coefficient was somewhat increased.

Comparison with theory.—Usually any large discrepancies between the lift of a wing and that predicted from inviscid fluid theory can be attributed to flow separation. Since the application of boundary-layer control should reduce the amount of flow separation, it is reasonable to assume that the lift obtained by the use of boundary-layer control should approximate that predicted by inviscid fluid theory. Figure 21 shows a comparison of the flap lift increments due to boundary-layer control obtained in this investigation with those estimated by the theory of reference 5.³ The experi-

³ The theoretical flap effectiveness was estimated from $\Delta C_L = \frac{d\alpha}{d\delta_f} C_{L\delta} \frac{\delta_f}{57.3}$ (equivalent to eq. (7), ref. 5)

For the F-56D wing

$$C_{L\delta} = 1.52 \text{ (from cross plot of fig. 5, ref. 5)}$$

$$\frac{d\alpha}{d\delta_f} = 0.58 \text{ (from curve for theoretical flap effectiveness, fig. 3, ref. 5. Average } c_f/c = 0.23 \text{ perpendicular to flap hinge line)}$$

$$\tan \delta_f = \cos A_f \tan \delta_r = 0.595 \tan \delta_r$$

$$\Delta C_L = \frac{(0.58)(1.52)}{57.3} \delta_f = 0.0154 \delta_f$$

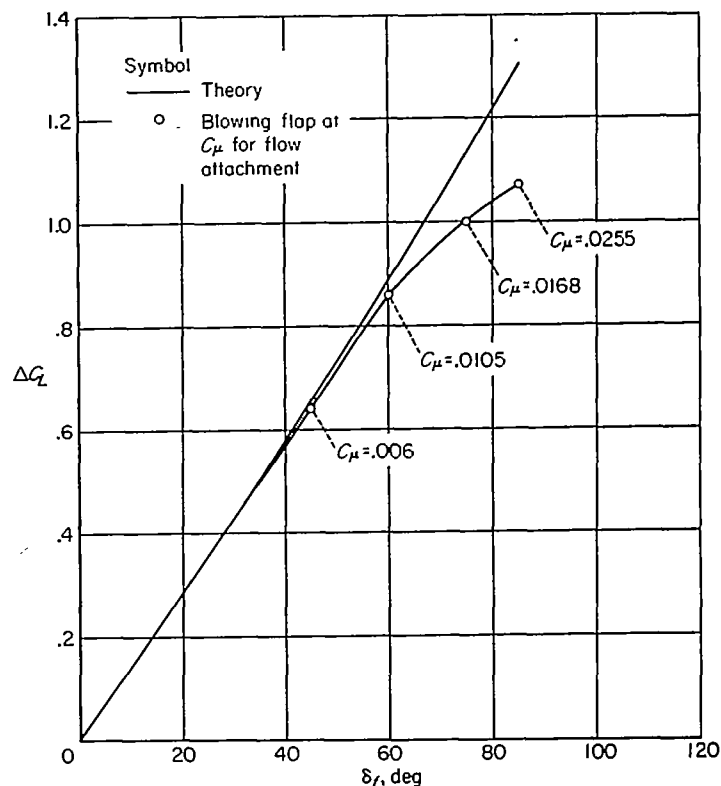


FIGURE 21.—Comparison of theoretical flap lift increments with those obtained experimentally on the blowing flap at the point of flow attachment; $\alpha = 0^\circ$.

mental flap lift increments chosen were those existing when the flow over the flap first became attached, as indicated by static-pressure measurements near the flap trailing edge. The momentum coefficients required to eliminate flow separation for each flap deflection are also presented. It may be seen by referring to figure 15(b) that these momentum coefficients are in the region where the rate of increase of lift coefficient with momentum coefficient falls off to a relatively low value. This affords an alternative, but often less precise, method of selecting the point of flow attachment. It may be seen from figure 21 that, for flap deflections up to 60° , the estimated and experimental flap lift increments are in good agreement. The discrepancies between the predicted and experimental values at higher flap deflections are believed to be due more to the linearizing assumptions utilized in the theory rather than to an actual deterioration of the flow over the flap. Even at a flap deflection of 85° the static-pressure measurements on the flaps indicated that attached flow was obtained.

FLIGHT TESTS

Aerodynamic characteristics with the 6-3 slatted leading edge.—Data are presented in figures 22 (a) and (b) for various flap deflections with blowing on and off for 100- and 80-percent engine rpm, and in figure 22 (c) for 60° flap deflection and various engine rpm's. The equations used to determine C_L and C_D are discussed in appendix A. The data in figure 22 indicate substantial increases in lift resulting from the application of blowing at all flap deflections. It will be noted that the angle of attack for maximum lift coefficient

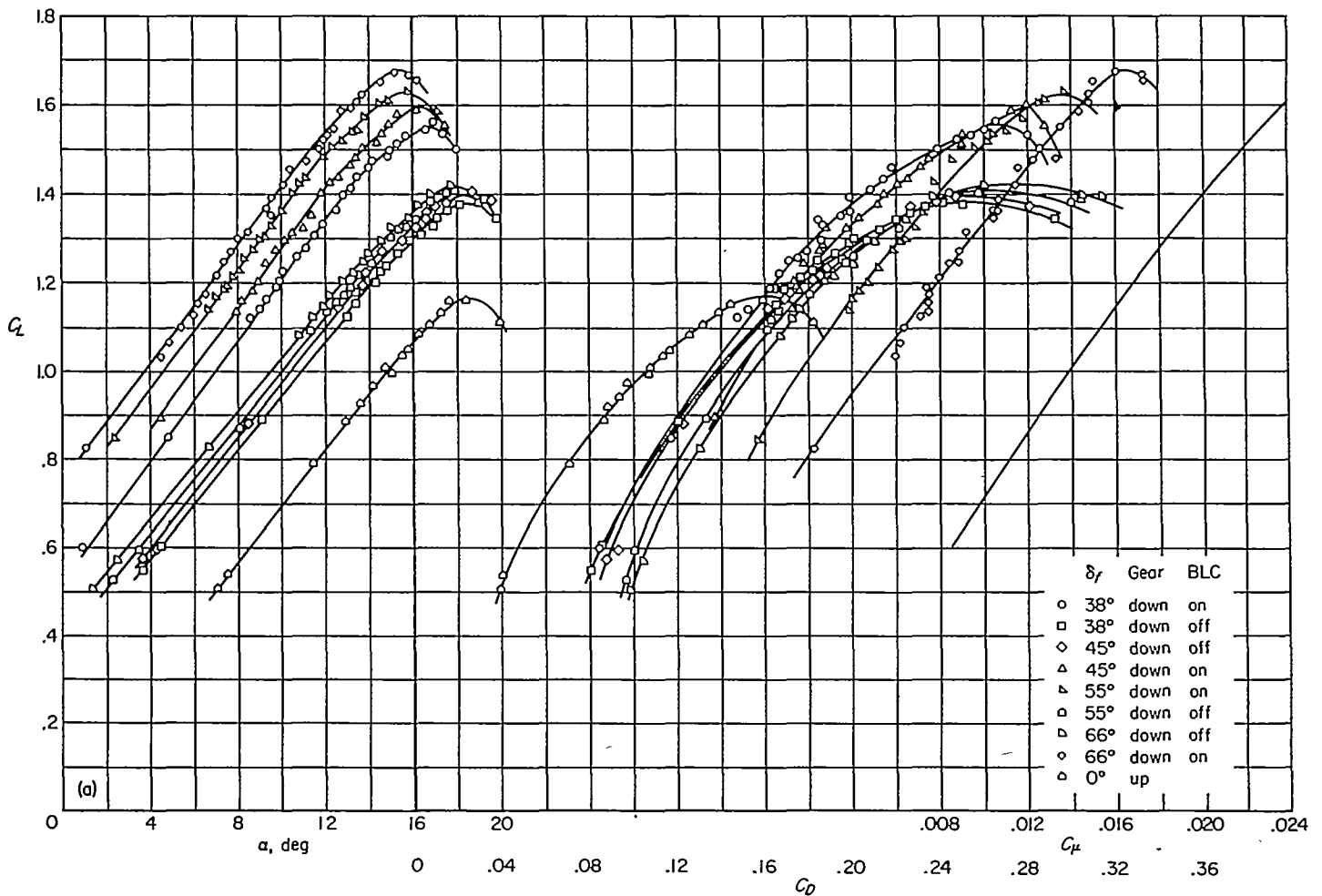
decreases with the amount of blowing, and with increase in flap deflection.

Flight tests of the airplane equipped with the standard 38° slotted flap normally used on this airplane gave essentially the same results as those shown for the plain flap deflected 38° without blowing. The improvement in C_L with blowing on the flaps deflected 55° over that obtained with the 38° flap was from 1.02 to 1.37 at the landing approach condition ($\alpha=11^\circ$, 80-percent rpm). With the flaps deflected 66°, there was an increase in $C_{L_{max}}$ from 1.40 to 1.68 at maximum engine power.

It can be observed from the data in figure 22 that the flap lift increment due to blowing varies over the angle-of-

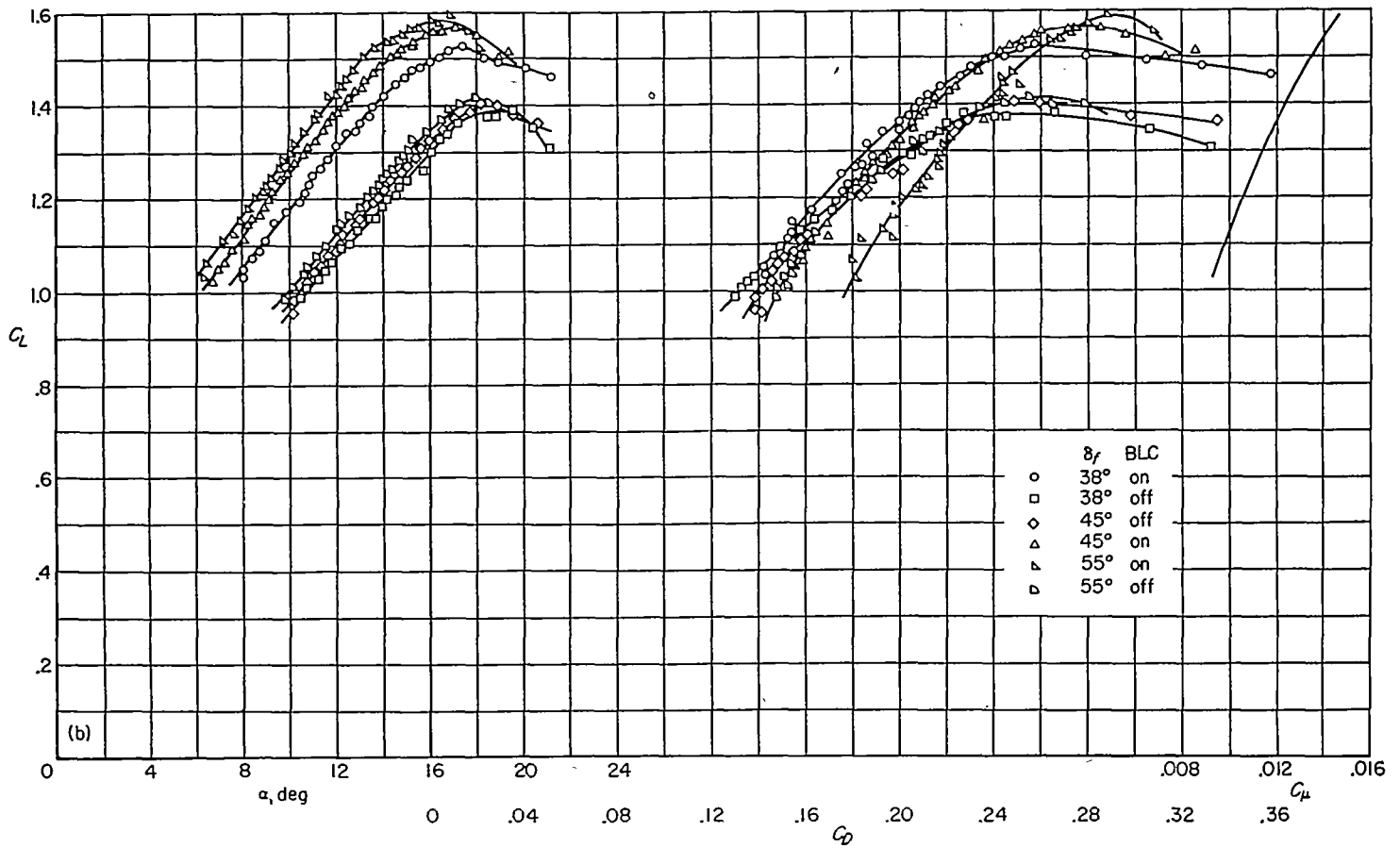
attack range. It is noteworthy that maximum flap lift increment occurs in the angle-of-attack range (10° to 12°) for the landing approach.

Aerodynamic characteristics with the standard F-86 leading-edge slats.—The lift and drag characteristics of the airplane equipped with the standard F-86 leading-edge slats are shown in figure 23. It is seen that, with blowing on, opening the leading-edge slats did not provide any increase in $C_{L_{max}}$. This same result was obtained in the wind-tunnel investigation. However, the leading-edge slats did improve the stalling characteristics of the airplane considerably.



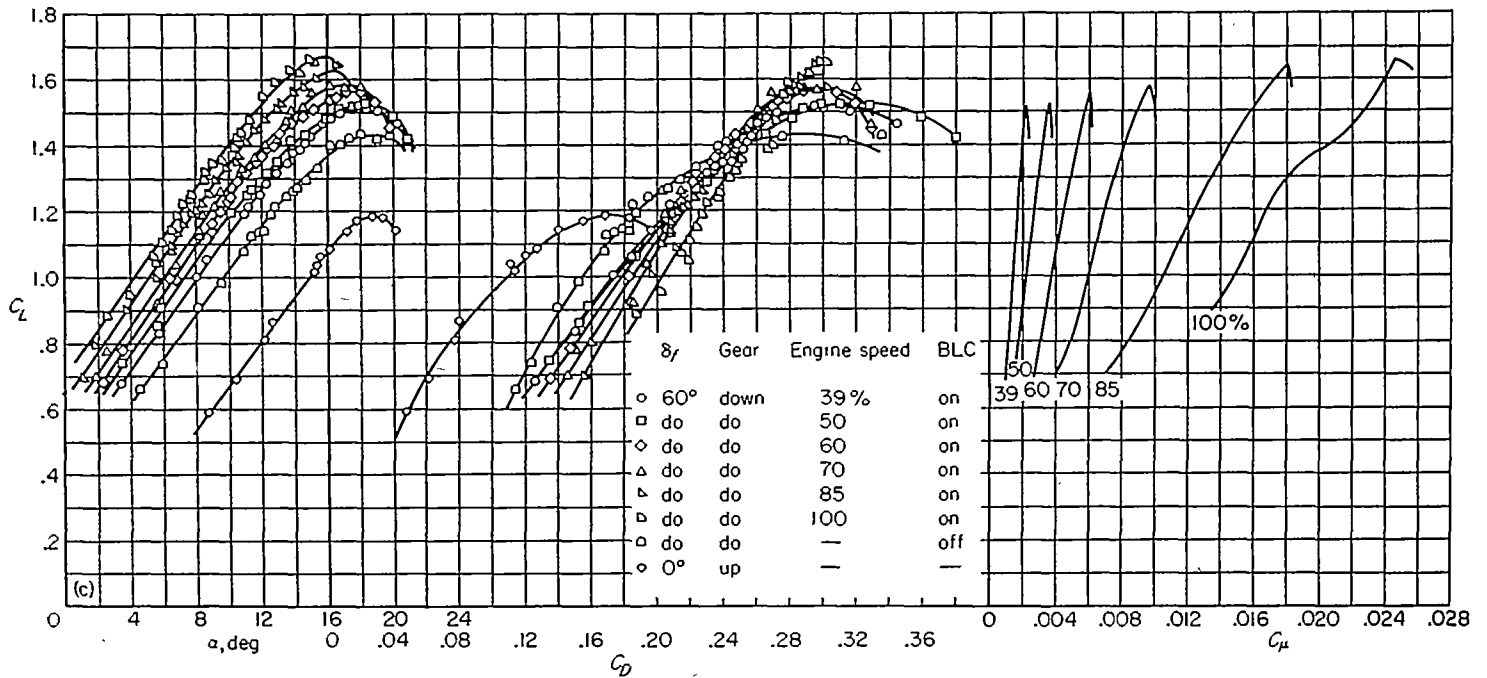
(a) 100-percent engine speed.

FIGURE 22.—Lift, drag, and momentum coefficient curves for various flap deflections; 6-3 slatted leading edge.



(b) 80-percent engine speed.

FIGURE 22.—Continued.



(c) $\delta_f=60^\circ$, various rpm.

FIGURE 22.—Concluded.

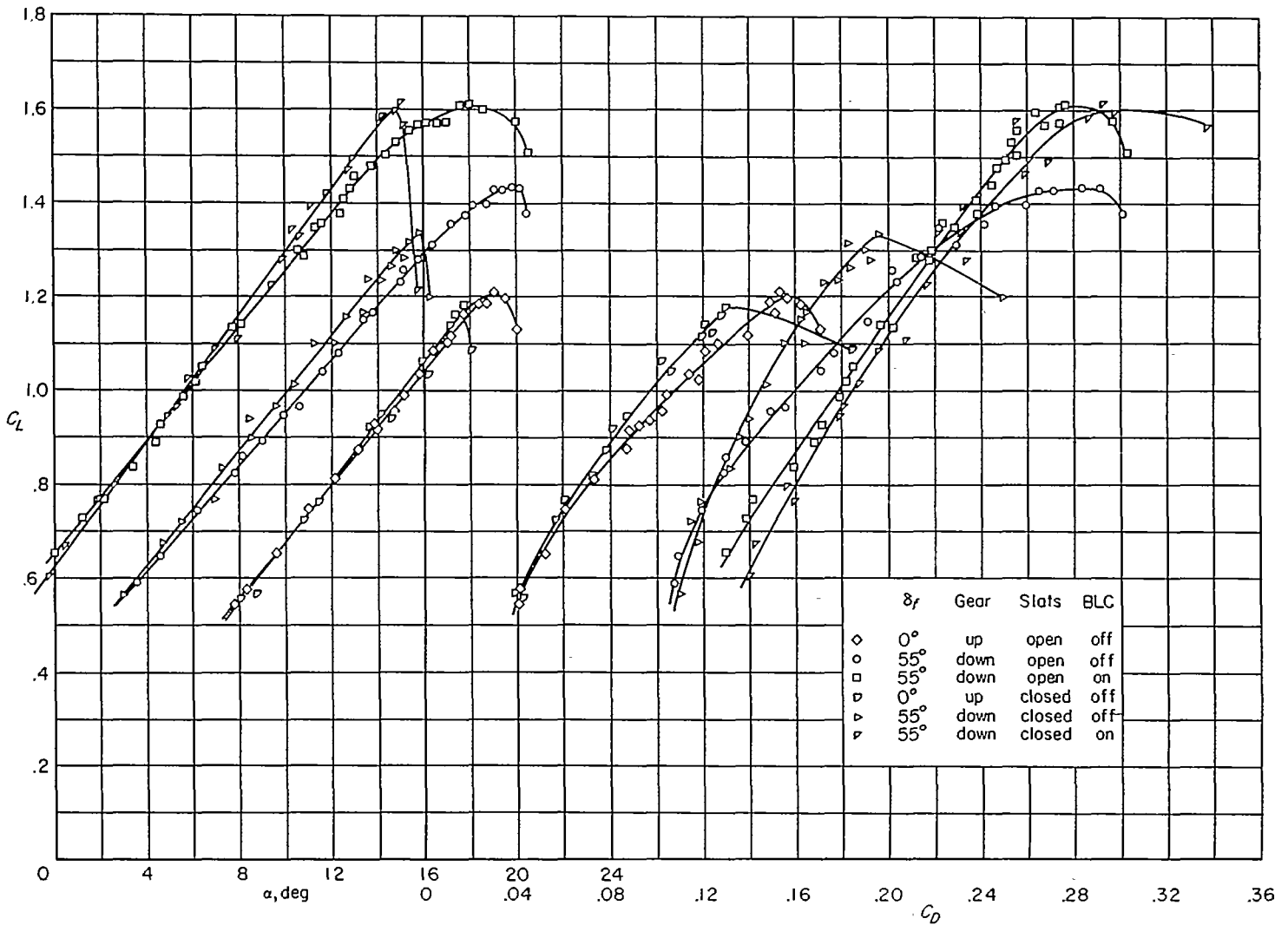


FIGURE 23.—Lift and drag curves for the airplane with the standard F-86D leading-edge slats; 80-percent engine speed.

Figure 24 shows a comparison between flight and wind-tunnel results for the flaps deflected 60° and at an angle of attack of 12°. The flight results are presented with the gear up to correspond to the configuration tested in the wind tunnel. These data show reasonably good correlation between the wind-tunnel results and the flight results over the C_μ range tested.

Pilot evaluation of the use of boundary-layer control.—A total of 48 flights were made by four Ames pilots, a number of company test pilots, and service pilots to evaluate the airplane with and without boundary-layer control. In particular, it was desired to know the effect of BLC on the landing-approach speeds, take-off characteristics, and flying qualities.

Approach speeds: The landing-approach speeds chosen by the NACA pilots for a carrier-type approach at 12,850 pounds, the stalling speeds, and the stalling characteristics are presented in table III for the airplane with various leading-edge devices for 55° flap deflection. Included in the table for comparison are the values for the slotted flap ($\delta_f=38^\circ$).

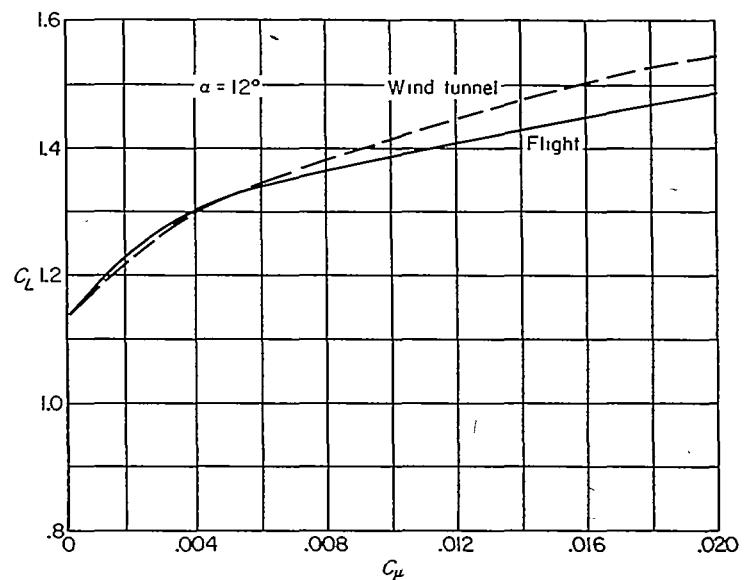


FIGURE 24.—Comparison of wind-tunnel and flight results; F-86D slatted leading edge, $\delta_f=60^\circ$, gear up.

These data indicate that substantial reductions in approach speed are realized with the boundary-layer control operating. For the normal type slatted leading edge, a 12-knot reduction in average approach speed over the slotted flap was obtained, while a 9-knot reduction was obtained with the 6-3 slatted leading edge. The variation of average approach speed with gross weight with the 6-3 leading edge for the 55° flap deflection, blowing on and off, and the slotted flap is presented in figure 25. These data were computed on the assumption that the pilot would approach at the same angle of attack regardless of gross weight.⁴

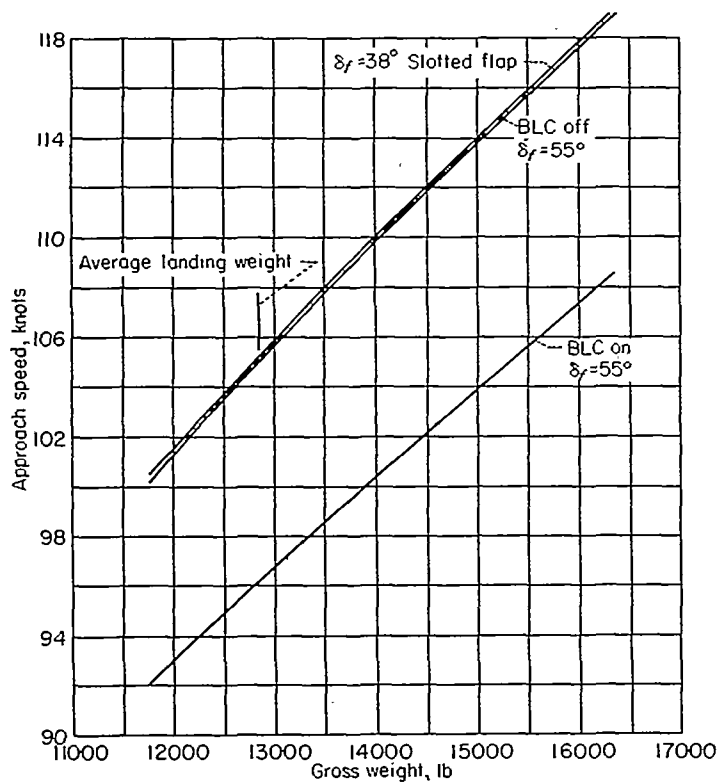


FIGURE 25.—Variation of approach speed with gross weight for various flap deflections; 6-3 slatted leading edge.

The reasons given by the pilots for selecting a minimum comfortable approach speed changed in most cases from the ability to arrest a sink rate or to control altitude without boundary-layer control to proximity to the stall with boundary-layer control on. The relationship between the pilots' selected approach speeds and the lift curves for the airplane with the 6-3 slatted leading edge is given in figure 26. These data indicate that the pilots did not make approaches at the same angle of attack with blowing on and off. Although the pilots felt that the ability to control altitude while maintaining a desired approach airspeed was greatly improved with blowing on, a reduction in angle of attack was necessary to maintain a safe margin below maximum lift.

Each pilot also made carrier approaches with the flaps deflected 66°. In this case the increased lift resulted in only small (1 to 2 knots) reductions in approach speed. The 66° flap deflection was not felt to be desirable for carrier ap-

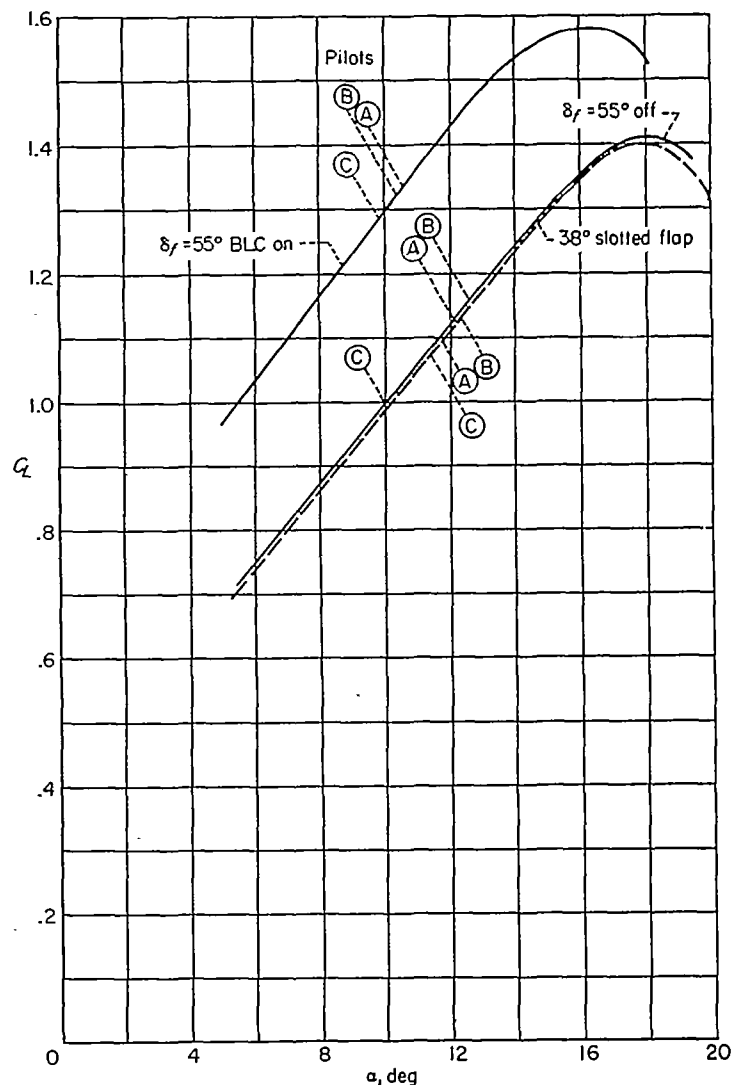


FIGURE 26.—Relationship of pilot's selected approach speeds to lift curves for various flap deflections; 6-3 slatted leading edge, 80-percent engine speed, $W/S=42.5$, $\delta_f=55^\circ$.

proaches because of the increased drag causing poorer wave-off performance.

The foregoing discussion has been concerned with carrier-type approaches which are made at essentially constant altitude with power for level flight. For normal field operation, a sinking-type approach is used at reduced engine powers. Because engine power has a direct effect on the amount of flap lift produced with blowing on, as well as affecting the steepness of the glide path, the approach speeds selected in a sinking-type approach will vary, depending on the amount of power used. The effect of engine power on flap lift increment is indicated by the data presented in figure 27 for a 55° flap deflection. The data show a smooth variation of flap lift with rpm. Figure 28 shows the variation of selected approach speed with engine rpm for a 55° flap deflection with boundary-layer control on and off. These approaches were made at constant power and constant airspeed with the throttle retarded after the flare (except for idle condition). Although an appreciable amount of lift due to blowing is present even at idle power, the data in figure 28 indicated that if the entire approach is made near idle power,

⁴ Several pilots commented on the improvement in turning performance during landing approach by noting an increase in attainable angle of bank or normal acceleration with blowing on.

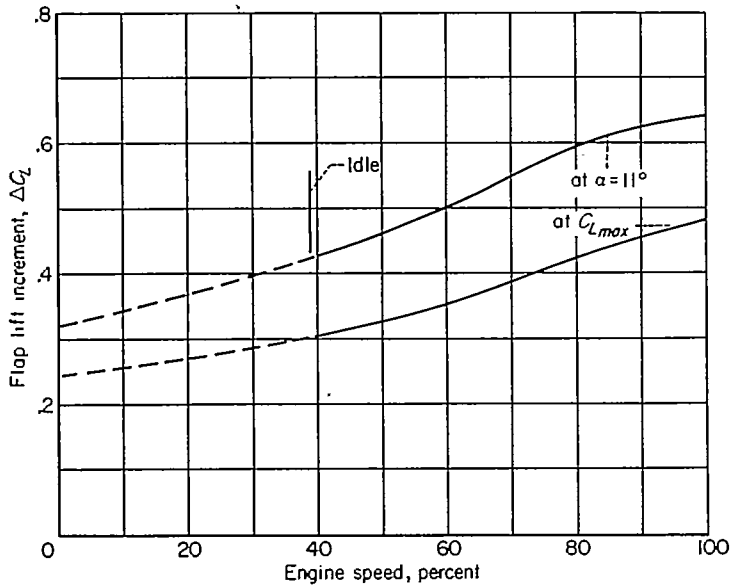


FIGURE 27.—Variation of flap lift increment with engine speed; 6-3 slatted leading edge, $\delta_f=55^\circ$.

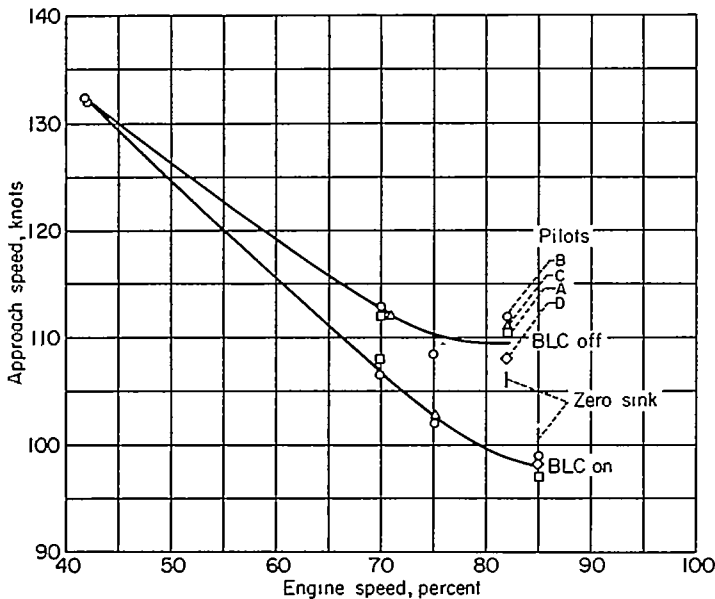


FIGURE 28.—Effect of engine speed on approach speed; blowing off and on, $\delta_f=55^\circ$, 6-3 slatted leading edge, sinking-type approach.

little or no reduction in approach speed would be realized. It should be noted that for modern jet-powered aircraft, approaches rarely are made at idle power. With the low values of L/D characteristic of modern aircraft, it is necessary in the interest of safety to use moderate amounts of engine power to prevent excessively high sink rates and provide satisfactory engine response in case of a wave-off. If idle power approaches are necessary for a particular design, a larger nozzle gap could be used to provide the required C_{μ} values. There should be incorporated, however, a means of reducing the flow to avoid unnecessary loss of engine thrust at higher values of engine power. In order to get the maximum utilization of the boundary-layer control for a sinking-type approach, the NACA pilots modified their approach and used lower power to reduce airspeed and lose altitude in the early part of the landing pattern, and then

increased power in the final approach, with a cut in power after the flare. Final approach speeds for landings made in this manner could be as slow as those obtained in the carrier-type approaches. In an approach where 70-percent rpm was maintained until the landing flare was initiated, due to windmilling action, the engine rpm dropped off only to 55 percent at touchdown. For the sinking-type approach, some pilots preferred a 66° flap deflection since the added drag permitted higher engine rpm and resulted in improved engine response and increased lift due to blowing.

In regard to instrument-type landings, several pilots commented that with blowing the airplane was held more easily at a desired approach speed. This effect is presumably tied in with the increased slope of the C_L-C_D curve with blowing on which results in smaller drag changes for a given lift change.

In order to investigate further the action of boundary-layer control in sinking-type approaches, several GCA (ground control approach) approaches were made using the Moffett Field GCA facilities. The pilot's comments were as follows:

"The first approach was made attempting to use the technique described in the pilot's handbook (i. e., power constant at 78 percent, 150 knots, on level portion of final approach, and upon reaching glide slope, opening speed brakes which is supposed to result in 500 feet per minute rate of descent at 150 knots). The flaps were set at 38° , blowing off. Altitude control was good; however, it seemed rather difficult to maintain the desired airspeed and a number of power corrections had to be made. Even so, rather large excursions from the desired airspeed occurred (10 to 15 knots). The second approach was made with 55° flap deflection with boundary-layer control off. The entire approach was made at 130 knots which seemed quite comfortable. Power required was about 80 percent, speed brakes were opened upon reaching the glide slope. In general, it seemed easier to hold close to the desired airspeed. Altitude control again was good. Two approaches were then made with the boundary-layer control on. On the first the flap deflection was left at 55° throughout the approach and the speed brakes were opened to start the rate of descent. On the second, 55° flap deflection was used to the glide slope, at which point the flaps were lowered to 66° , leaving the speed brakes retracted. This latter procedure seemed the most effective in commencing the 500 feet per minute rate of descent. The desirable approach speed seemed to be 115 knots which required about 83-percent rpm. Speed control with boundary-layer control on was excellent. Glide slope corrections were easily made with little effort, requiring only slight changes in power. Once the correct power and rate of descent were established the airplane seemed to ride down the glide slope as if it were on a track."

Other pilots made comments relative to the take-off characteristics. The fact that additional lift was available with no change in airplane attitude when the blowing was turned on was appreciated by some pilots and was felt to be desirable for instrument-type take-offs. Because of the high drag above 110 knots, a modified climb-out technique

was used to get maximum performance (i. e., climb initially at 100 to 110 knots, then turn the boundary-layer control off before acceleration to higher speeds).

Flying qualities: The following discussion will cover those items on which boundary-layer control had an effect. All other flying qualities were unaffected by boundary-layer-control operation.

The longitudinal trim changes due to the operation of the boundary-layer-control system on this airplane were considered to be excessive by the pilots. The measured control forces are presented in the following table:

Longitudinal stick force, lb	Initial trim condition					Configuration change	Parameter to be held constant
	Speed, knots	Gear	Flaps	Power, percent	BLO		
0	140 (1.4 V_{st})	Down	Up	80	Off		
7 pull	140	Down	55° down	80	Off	Flaps down	Altitude
18 pull	140	Down	55° down	87	On	BLO on	Altitude
0	140	Up	55° down	100	On		
15 push	-----	Up	55° down	100	Off	BLO off	Rate of climb
24 push	-----	Up	Up	100	Off	Flaps up	Rate of climb

Although the trim changes noted in the table are large, it is not felt that the boundary-layer-control operation in itself would represent a serious trim change problem. It can be noted that large trim changes were encountered in operation of the flaps alone and result from the type of force feel system (irreversible control system with a bungee-fixed spring gradient picked on the basis of high-speed flight) employed on this airplane. It is of interest to note that the pitching-moment change with the application of blowing measured in the wind tunnel for the F-86D airplane was in an opposite direction to that measured in flight in the present investigation. The reason for this is felt to be due to the difference in horizontal tail geometry between the two airplanes.

The effect of the boundary-layer control on the stalling characteristics was dependent somewhat on the type of leading-edge device employed with it. For the 6-3 slats and the slotted flap ($\delta_f=38^\circ$) the stall was characterized by a mild pitch-up coupled with a lateral unsteadiness which was controllable. The pitch-up was followed by a pitch-down. There was no stall warning. The stall in this configuration was considered satisfactory. With the plain flap deflected 55° and boundary-layer control off, the pitch-up was more pronounced. Applying boundary-layer control tended to increase the pitch-up and the stall itself was considered marginal to unsatisfactory due chiefly to the poor stall recovery characteristics. In order to recover from the stall, large forward stick displacements were necessary and the associated stick forces were objectionable. The pitch-up at the stall and the poor stall recovery characteristics were aggravated by the extreme rearward center-of-gravity location (approximately 27 percent) with the 6-3 slats installed. With the F-86D slats, the stall was considered satisfactory for all conditions; however, the application of boundary-layer control tended to reduce the stall warning and render it marginal to unsatisfactory.

Operational characteristics: In the evaluation of the performance of the airplane, actual measurements of landing and take-off distances, climb, and catapult launching were not made; but by the use of the lift and drag data obtained with the 6-3 slatted leading edge and engine thrust data, computations have been made of the performance. The methods used for computing performance are contained in appendix B and are felt to be adequate for comparative purposes.

Landing performance: The landing distance over a 50-foot obstacle and the ground roll distance were computed

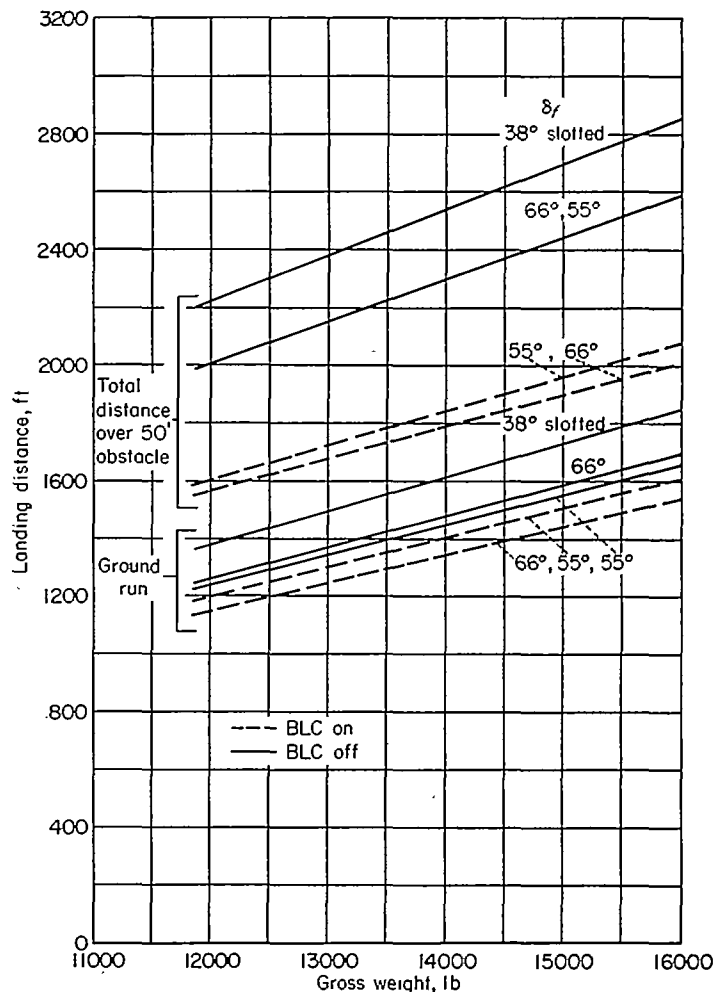


FIGURE 29.—Variation of landing distance with gross weight for various flap deflections; 6-3 slatted leading edge, sea level.

for the landing configuration using the average approach speeds selected by the pilots and are presented in figure 29 for flap deflections of 55° and 66° , blowing on and off. For comparison purposes the computed distances for the normal 38° slotted flap deflection are also presented in figure 29. These data indicate that a reduction of approximately 30 percent in total distance would be realized using the 66° flap deflection with blowing on at an airplane gross weight of 14,000 pounds.

Take-off performance: In the computations for take-off and climb, account is taken of the thrust loss incurred as a result of extracting air from the engine compressor. In order to operate the engine within the allowable tail-pipe tempera-

ture when extracting air for boundary-layer control, a reduced value of rpm is used. The thrust reduction was approximately 270 pounds at maximum power.

In considering a *catapult type take-off* this reduction in thrust is not too significant, since take-off acceleration is provided principally by the catapult itself. It is required, however, that sufficient engine thrust be available to accelerate the airplane after launch with a minimum longitudinal acceleration of approximately 0.065g.⁵ Lift-off speed is selected as the speed at nine-tenths of $C_{L_{max}}$ or at the maximum ground attitude. The results of computations of the take-off speeds at the end of the catapult run as a function of gross weight for various flap deflections with blowing on and off are presented in figure 30. Indicated in this figure

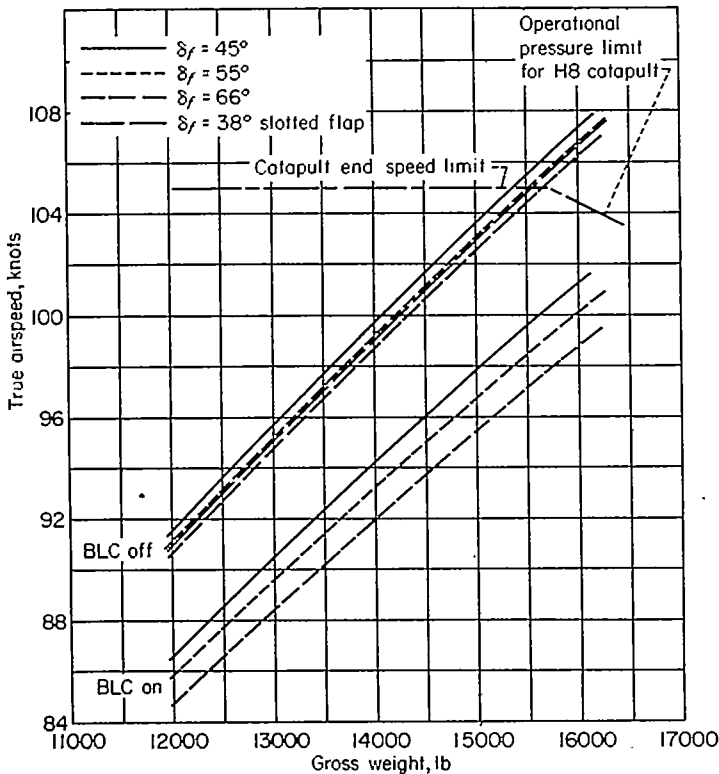


FIGURE 30.—Variation of catapult take-off velocity with gross weight for various flap deflections with blowing on and off; 6-3 leading edge, sea level.

are the H8-catapult characteristics. The results indicate significant improvements in performance with blowing on. Compared to the 38° deflection of the slotted flap, the 66° deflection of the flap with boundary-layer control would allow an 8-knot reduction in catapult take-off speed at a gross weight of 16,000 pounds. At this gross weight the longitudinal acceleration would be approximately 0.15g.

With regard to a *field take-off*, the assumption is made that the airplane accelerates on the ground in a level attitude, and at take-off speed the airplane is rotated to the angle of attack corresponding to a velocity of 1.2 V_s . For the transition distance, it is assumed that the airplane is in a steady rate of climb at the value for the 50-foot-height point. The results of the computations presented in figure 31 indicate

⁵ Assumed minimum acceleration value used to assure that the airplane does not sink after launch.

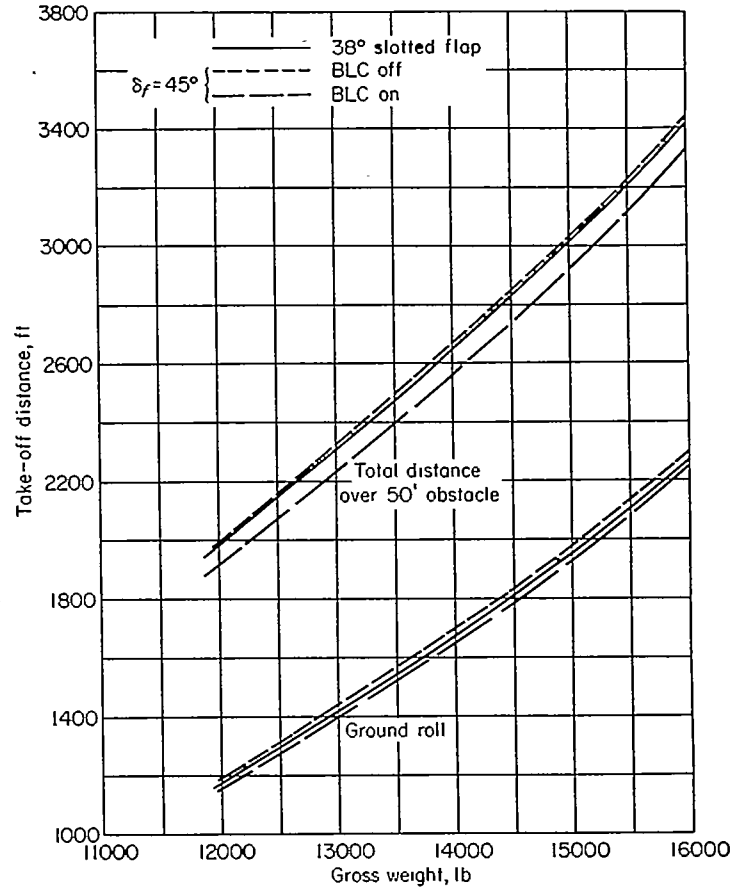


FIGURE 31.—Variation of take-off distance with gross weight for various flap deflections; blowing on and off, 6-3 slatted leading edge, sea level.

small improvements in total distance over a 50-foot obstacle with blowing on for the 45° flap deflection compared with the standard 38° slotted flap. The take-off performance was computed with the maximum possible C_μ available. Reducing the air flow to the flaps to reduce the thrust loss and thus operate at a lower C_μ made a further improvement in the take-off performance. By waiting until take-off speed is reached before turning on the boundary-layer control, a further reduction of 6 percent would be realized.

Climb characteristics: The rate of climb after a catapult take-off (at a speed of 1.05 V_s) is presented as a function of gross weight in figure 32. Although the rate of climb is reduced when blowing is used, it should be kept in mind that because of the lower stalling speed it is possible to climb at a lower airspeed with blowing on so that there is no significant change in climb angle.

SUMMARY OF RESULTS AND CONCLUSIONS

The following conclusions are based on wind-tunnel and flight investigations of F-86 type aircraft with blowing boundary-layer control on the trailing-edge flaps:

1. Correlation of flap lift with jet momentum coefficient was good for the range of pressure ratios obtainable from turbojet engine bleed air systems.
2. The lift increment obtained by preventing flow separation on the flap can be predicted up to 60° flap deflection by the linear inviscid fluid theory of NACA Rep. 1071.

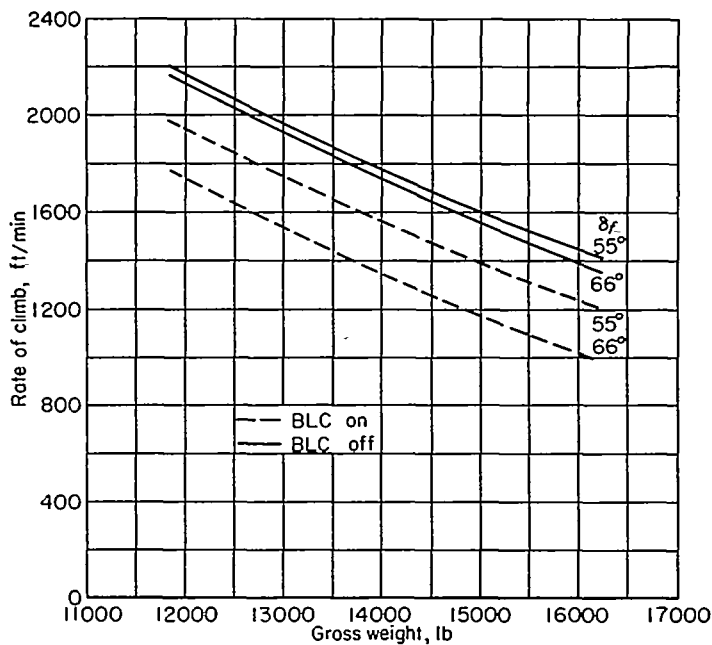


FIGURE 32.—Variation of rate of climb with gross weight for various flap deflections with blowing on and off; wave-off speed = 1.0517, 6-3 leading edge, sea level.

3. Higher lift increments than those obtained by preventing flow separation on the flaps can be achieved by further increasing the momentum coefficient to values above that required to prevent flow separation. However, once the flow is attached to the flap, large values of momentum coefficient are required to increase the lift significantly.

4. Lateral stability was increased slightly by blowing over the flaps, and the maximum roll power of the ailerons was increased by about 25 percent.

5. When the blowing nozzle was located in the upper surface of the flap, it was found that the chordwise position of the nozzle could be anywhere between the minimum

pressure point on the flap and the wing-flap juncture without seriously affecting the flap lift. If the nozzle is located too far downstream of the minimum pressure point, large losses in flap lift may result.

6. When the blowing nozzle was located in the wing shroud ahead of the flap, it was necessary to position the flap close to the nozzle to obtain the same lift coefficients at low momentum coefficients as those for the plain-blowing-flap configuration.

7. The blowing flap lift is relatively insensitive to spacers or structural members in the nozzle throat. It is also insensitive to flow disturbances such as those caused by leading-edge slats.

8. Blowing with the flaps deflected 55° reduced the average approach speed by as much as 12 knots in a carrier-type approach compared to the slotted flap deflected 38°. In sinking-type approaches smaller reductions in speed were realized.

9. Blowing with the flaps deflected 66° reduced the calculated landing distance by 30 percent compared to the standard 38° slotted flap. In takeoff performance calculations, the catapult end speed required at a given gross weight was reduced by 8 knots due to blowing. For a field-type takeoff the gains calculated were relatively small.

10. Improvements were noted by the pilots in control of the glide path with blowing on. Improvements were noted also in take-off since the airplane would tend to fly off without as much rotation in attitude required.

11. The longitudinal trim changes due to flap deflection and application of blowing were considered excessive by the pilots.

12. In some cases the stalling characteristics were made less desirable with blowing on.

AMES AERONAUTICAL LABORATORY

NATIONAL ADVISORY COMMITTEE FOR AERONAUTICS

MOFFETT FIELD, CALIF., April 30, 1958

APPENDIX A

EQUATIONS USED FOR DETERMINING LIFT AND DRAG

The equations used to determine the lift coefficients and drag coefficients are as follows:

$$C_L = \frac{W}{qS} (A_n \cos \alpha + A_x \sin \alpha) - \frac{1}{qS} (F_G \sin \alpha)$$

$$C_D = \frac{W}{qS} (A_n \sin \alpha - A_x \cos \alpha) + \frac{1}{qS} (F_G \cos \alpha - wV)$$

where

$\frac{W}{S}$	airplane wing loading, lb/sq ft
q	dynamic pressure, lb/sq ft
A_n	normal acceleration factor, g units
A_x	longitudinal acceleration factor, g units
α	angle of attack, deg
w	engine air flow, lb sec/ft
V	free-stream velocity, ft/sec
F_G	engine gross thrust, lb

APPENDIX B

METHODS USED FOR PERFORMANCE EVALUATION

The following equations and assumptions were used in computing the performance:

Landing distance:

$$\text{Air distance} = \left(\frac{V_{50}^2 - V_L^2 + 50}{64.4} \right) \frac{L}{D}, \text{ ft}$$

(ref. 7, p. 198) where V_{50} is pilots' average approach speed and the landing velocity

$$V_L = 1.05V_s$$

$$\text{Ground run} = \frac{V_L^2}{64.4[\mu - (D/L)]} \log e \left(\frac{L}{D} \right) \mu, \text{ ft}$$

and $\mu = 0.4$ (ref. 8, p. 312).

Take-off distance:

$$\text{Ground run} = \frac{WV_{TO}^2}{64.4[T - \mu W - Sq(C_D - \mu C_L)]}, \text{ ft}$$

(from ref. 7, pp. 195-196)

$$\text{Air distance} = \frac{50W}{T-D} + \frac{V_{TO}^2}{g\sqrt{2}}, \text{ ft}$$

(ref. 9, p. 51) where take-off velocity

$$\begin{aligned} V_{TO} &= 1.2V_s \\ &= 1.2\sqrt{\frac{843(W - T \sin \alpha)}{SC_{L_{max}}}}, \text{ ft/sec} \end{aligned}$$

and

T	thrust at 100-percent engine speed
q	$\frac{\rho}{2} (0.7V_{TO})^2$
W	airplane gross weight in pounds
α	angle of attack at $C_{L_{max}}$ or at maximum ground angle
μ	0.02

(The assumption is made that steady climb has been attained before reaching the 50 foot height.)

Catapult end speed:

$$V_{TO} = \sqrt{\frac{295(W - T \sin \alpha_{TO})}{SC_{L_{TO}}}}, \text{ knots}$$

where

$C_{L_{TO}}$	$0.9C_{L_{max}}$
α_{TO}	angle of attack at $C_{L_{TO}}$

Climb:

$$\text{Rate of climb} = \frac{60V_c(T-D)}{W}, \text{ ft/sec}$$

where

V_c	$1.05V_s$, ft/sec
T	thrust at climb power
D	drag at V_c

REFERENCES

- Schwieber, W.: Lift Increase by Blowing Out Air, Test on Airfoil of 12 Percent Thickness, Using Various Types of Flap. NACA TM 1148, 1947.
- Schwieber, W.: Lift Increase Produced by Blowing a Wing of a Profile Thickness of 9 Percent Equipped with a Slat and a Slotted Flap. Air Materiel Command Trans. Rep. F-TS-645-RE, Sept. 1946. (See also: R-30-18, pt. 9 (Ger-207), Goodyear Aircraft Corp. Trans. from: (ZWB, Berlin, FB 1622).
- Harkleroad, E. L., and Murphy, R. D.: Two-Dimensional Wind-Tunnel Tests of a Model of an F9F-5 Airplane Wing Section Using a High-Speed Jet Blowing Over the Flap: Part I—Tests of a 6-Foot Chord Model. David Taylor Model Basin Aero. Rep. 845, May 1953.
- Kelly, Mark W., and Tucker, Jeffrey H.: Wind-Tunnel Tests of Blowing Boundary-Layer Control With Jet Pressure Ratios Up to 9.5 on the Trailing-Edge Flaps of a 35° Sweptback Wing Airplane. NACA RM A56G19, 1956.
- DeYoung, John: Theoretical Symmetric Span Loading Due to Flap Deflection for Wings of Arbitrary Plan Form at Subsonic Speeds. NACA Rep. 1071. (Supersedes NACA TN 2278.)
- Cook, Woodrow L., Holzhauser, Curt A., and Kelly, Mark W.: The Use of Area Suction for the Purpose of Improving Trailing-Edge Flap Effectiveness on a 35° Sweptback Wing. NACA RM A53E06, 1953.
- Perkins, Courtland D., and Hage, Robert E.: Airplane Performance, Stability and Control. John Wiley & Sons, Inc., 1949.
- Dwinnell, James H.: Principles of Aerodynamics. McGraw-Hill Book Co., 1949.
- Lush, Kenneth J.: Standardization of Take-Off Performance Measurements for Airplanes. Tech. Note R-12, Edwards Air Force Base, Edwards, California (1954).

TABLE I.—COORDINATES OF THE WING AIRFOIL SECTIONS NORMAL TO THE WING QUARTER-CHORD LINE AT TWO SPAN STATIONS

[Dimensions given in inches]

Section at 0.467 semispan			Section at 0.857 semispan		
Distance from L. E.	Ordinate		Distance from L. E.	Ordinate	
	Upper	Lower		Upper	Lower
0	0.231	-----	0	-0.098	-----
.119	.738	-0.307	.089	.278	-0.464
.239	.943	-.516	.177	.420	-.605
.398	1.127	-.688	.295	.562	-.739
.597	1.320	-.895	.443	.701	-.879
.896	1.607	-1.196	.738	.908	-1.089
1.092	2.104	-1.703	1.476	1.273	-1.437
3.884	2.715	-2.358	2.952	1.730	-1.878
5.976	3.121	-2.811	4.428	2.046	-2.176
7.968	3.428	-3.161	5.903	2.290	-2.401
11.952	3.893	-3.687	8.855	2.648	-2.722
15.936	4.157	-4.064	11.806	2.911	-2.944
19.920	4.357	-4.364	14.758	3.104	-3.102
23.904	4.480	-4.573	17.710	3.244	-3.200
27.888	4.533	-4.719	20.661	3.353	-3.250
31.872	4.525	-4.800	23.613	3.380	-3.256
35.856	4.444	-4.812	26.564	3.373	-3.213
39.840	4.299	-4.758	29.516	3.322	-3.128
43.824	4.081	-4.638	32.467	3.219	-2.989
47.808	3.808	-4.452	35.419	3.074	-2.803
51.792	3.470	-4.202	38.370	2.885	-2.574
55.776	3.068	-3.891	41.322	2.650	-2.302
59.760	2.603	-3.521	44.273	2.374	-1.986
63.744	2.079	-3.080	47.225	2.054	-1.625
63.681	-.740	-----	63.031	.321	-----

L. E. radius: 1.202, center at (1.201, 0.216) L. E. radius: 0.822, center at (0.822, -0.093)

* Straight lines to trailing edge.

TABLE II.—DIMENSIONS OF TEST AIRPLANE

Wing:	
Total area, sq ft (with F-88D-type slats)	287.9
Total area, sq ft (with extended leading edge)	302
Span, ft	37.12
Aspect ratio	4.79
Taper ratio	0.51
Mean aerodynamic chord (wing station 98.7 in.), ft	8.1
Dihedral angle, deg	3.0
Sweepback of 0.25-chord line, deg	35.23
Geometric twist, deg	2.0
Root airfoil section (normal to 0.25-chord line)	NACA 0012-64 (modified)
Tip airfoil section (normal to 0.25-chord line)	NACA 0011-64 (modified)
Wing area affected by flap, sq ft	116.0
Horizontal tail:	
Total area, sq ft	35.0
Span, ft	12.7
Aspect ratio	4.65
Taper ratio	0.46
Dihedral angle, deg	10.0
Mean aerodynamic chord (horizontal-tail station 33.64 in.), ft	2.9
Sweepback of 0.25-chord line	34.68
Airfoil section (parallel to center line)	NACA 0010-64
Vertical tail:	
Total area, sq ft	34.4
Span, ft	7.5
Aspect ratio	1.74
Taper ratio	0.36
Sweepback of 0.25-chord line, deg	35.00
Flap:	
Total area, sq ft	23.7
Span (from 13.4 to 49.5-percent semispan), ft	7.27
Chord (constant), ft	1.07

TABLE III.—PILOTS' OBSERVED STALLING AND APPROACH CHARACTERISTICS FOR VARIOUS FLAP AND LEADING-EDGE DEVICES

Pilot	Configuration			Stall			Carrier approach 12,850 lb	
	Leading edge	Flap	BLO	Indicated air speed, knots	Gross weight, lb	Characteristics	Indicated air speed, knots	Reason for limiting approach speed
A	6-3 slat	38° slotted	None	89	12,760	Warning: Unsatisfactory Stall: No comment	105	Inadequate longitudinal control and visibility
	6-3 slat	55°	On	85	12,630	Warning: None—unsatisfactory Stall: Marginal—satisfactory	95	Proximity to stall, inadequate altitude control
	6-3 slat	55°	Off	90	12,720	Warning: None—unsatisfactory Stall: Marginal—satisfactory	103	Proximity to stall, inadequate altitude control and visibility
	F-86D slat	38° slotted	None	96	14,200	Warning: Satisfactory Stall: Satisfactory	106	Inadequate longitudinal control and visibility
	F-86D slat	55°	On	88	12,860	Warning: 93 knots, less than with BLO off Stall: Satisfactory	98	Proximity to stall
	F-86D slat	55°	Off	93	12,860	Warning: 103 knots, satisfactory Stall: Satisfactory	111	Inadequate longitudinal control and ability to arrest sink
B	6-3 slat	38° slotted	None	90	12,470	Mild pitch-up with roll-off	103-108	Proximity to pitch-up and roll-off
	6-3 slat	55°	On	86-88	12,860	Warning: Unsatisfactory Stall: Marginal, stall recovery unsatisfactory, mild pitch-up with lateral instability at $C_{L_{max}}$	93-98	Proximity to pitch-up
	6-3 slat	55°	Off	93	12,860	Warning: Unsatisfactory Stall: Marginal, satisfactory	98-103	Proximity to pitch-up
	F-86D slat	38° slotted	None	92	12,860	Warning: Satisfactory Stall: Satisfactory	103	Ability to arrest rate of sink, visibility
	F-86D slat	55°	On	88	12,860	Warning: 91 knots, satisfactory Stall: Satisfactory	96-98	Ability to control rate of sink
	F-86D slat	55°	Off	92	12,860	Warning: 96 knots; very mild; unsatisfactory Stall: Satisfactory	108-113	Ability to control rate of sink
C	6-3 slat	38° slotted	None	92	13,310	Smooth to 100 knots; yaw to left at 98 knots and fall through at 94 knots	106	Inadequate altitude control and proximity to stall
	6-3 slat	55°	On	86	12,860	Warning: Unsatisfactory Stall: Unsatisfactory due to pitch-up	97	Proximity to pitch-up
	6-3 slat	55°	Off	92	12,860	Warning: Unsatisfactory Stall: Marginal due to pitch-up	110	Ability to arrest rate of sink
	F-86D slat	38° slotted	None	98	14,300	Warning: Satisfactory Stall: Satisfactory	110	Ability to control rate of sink
	F-86D slat	55°	On	88	12,860	Stall: Satisfactory	98-100	Proximity to stall
	F-86D slat	55°	Off	92	12,860	Stall: Satisfactory	110-113	Ability to control altitude
D	F-86D slat	55°	On	90	12,960	Warning: 98 knots, unsatisfactory, light pitch-up Stall: Satisfactory	98	Inadequate altitude control
	F-86D slat	55°	Off	96	13,660	Warning: 99 knots, unsatisfactory Stall: No comment	108	Slow longitudinal control of flight path visibility

